

Analysis and Testing of Gelled, High Propulsive Green Propellant for Small Satellites in Low Earth Orbit

A project present to
The Faculty of the Department of Aerospace Engineering
San Jose State University

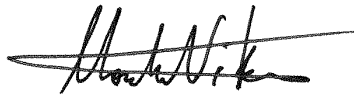
in partial fulfillment of the requirements for the degree
Master of Science in Aerospace Engineering

By

Stephen Lai

May 2015

approved by



Dr. Nikos Mourtos

Faculty Advisor



San José State
UNIVERSITY

© 2015
Stephen Lai
All Rights Reserved

Analysis and Testing of Gelled, High Propulsive Green Propellant for Small Satellites in
Low Earth Orbit

by
Stephen E. Lai

APPROVED FOR THE DEPARTMENT OF AEROSPACE ENGINEERING
SAN JOSE STATE UNIVERSITY
May 2015



*Dr. Nikos J. Mourlas, Project Advisor
Department of Aerospace Engineering*

14 May 15

Date

Abstract

Future Skybox Imaging satellites with on board liquid propulsion have to be concerned with propellant slosh usually dealt with by implementing propellant management devices. One way to eliminate slosh and keep the propellant over the tank outlet is to add a thickener to the liquid to create a thixotropic gel. To mimic Skybox satellites' actual monopropellant LMP-103S, ammonium dinitramide is replaced with ammonium acetate to create a simulated propellant. A thickener is added to create a gel. NASA's Chemical Equilibrium with Applications program shows the LMP-103S gel has a beginning of life specific impulse of 231 seconds as opposed to the tabulated value of 235 seconds for the liquid, both using ECAPS's 1 newton thruster. Computational flow dynamics simulations conclude that the thickener increases the simulant's viscosity enough that propellant management devices are not necessary even during the mission's highest angular rate impulse of $15^\circ/\text{s}$. Flow observations along with pressure and mass flow rate measurements were inconclusive and the exit conditions or injector need to be redesigned to atomize the propellant more effectively in the combustion chamber. An overall propellant system mass savings of 1.19 kg was found when using the gelled LMP-103S monopropellant.

Acknowledgements

This project would not have been feasible or as thoroughly completed without the direction, time, and knowledge of the following people.

Jonny Dyer, Chief Engineer at Skybox Imaging, was the instrumental knowledge base and technical project advisor. The work performed here would not be as in depth without his guidance and know-how. He was also able to find funding within Skybox to buy components for testing. The support and direction went above and beyond what I was expecting during the entire academic year.

Randy Kirchner, SJSU Assistant Safety Coordinator, provided the lab space for testing and validation and repeatedly went out of his way to find all the materials essential to the liquid and gel simulant creation. It was incredibly helpful to have one point of contact at SJSU who could do everything as fast and efficient as he could. None of the testing would have been done without his substantial help and donations of time.

Abhra Dasgupta, SJSU AIAA President, battled to get me funding through AIAA. The generous help structuring the grant proposal and constant push to make the funding available allowed the testing to come to fruition in a timely manner. His openness to help surpassed all normal expectations.

Dr. Nikos Mourtos, SJSU Professor and Aerospace Program Director, kept me on time with project updates, presentations, and provided needed feedback when asked. He was able to get my project off the ground and headed in the right direction while pointing me to the correct points of contact. It was extremely beneficial to have him as a home base throughout the year.

1

Table of Content

1	INTRODUCTION.....	1
2	MOTIVATION.....	2
3	PROJECT OBJECTIVE AND REQUIREMENTS.....	2
4	PROJECT TIMELINE.....	3
5	LITERATURE OVERVIEW.....	3
5.1	LMP-103S.....	7
6	METHODOLOGY.....	10
7	PHYSICAL MODELING AND TESTBED.....	10
7.1	LMP-103S SIMULANT.....	10
7.1.1	<i>Simulant Selection.....</i>	<i>11</i>
7.1.2	<i>Liquid Simulant Creation.....</i>	<i>11</i>
7.1.3	<i>Simulant Testing and Validation.....</i>	<i>12</i>
7.1.4	<i>Gel Simulant.....</i>	<i>12</i>
7.1.5	<i>Gel Simulant Creation.....</i>	<i>14</i>
7.2	GEL DISADVANTAGES.....	15
7.3	PROPELLANT SYSTEM.....	16
7.3.1	<i>Thruster Performance.....</i>	<i>16</i>
7.3.2	<i>Pressure Levels.....</i>	<i>16</i>
7.3.3	<i>BOL/EOL Propellant Tank Pressure.....</i>	<i>17</i>
7.3.4	<i>Pressurant Gas.....</i>	<i>18</i>
7.3.5	<i>Throat Area and Mass Flow Rate.....</i>	<i>19</i>
7.4	PROPELLANT SYSTEM TESTBED.....	19
7.5	TESTBED RESULTS.....	22
7.5.1	<i>Liquid.....</i>	<i>22</i>
7.5.2	<i>Gel.....</i>	<i>25</i>
8	COMBUSTION.....	30
8.1	CHEMICAL EQUILIBRIUM WITH APPLICATIONS.....	30
8.2	COMBUSTION SIMULATION AND ANALYSIS.....	30

8.2.1	Combustion of Liquid LMP-103S.....	31
8.2.2	Combustion of Gel LMP-103S.....	32
8.3	COMBUSTION RESULTS.....	33
9	PROPELLANT MANAGEMENT DEVICES.....	33
9.1	SLOSH.....	33
9.2	ELIMINATION OF PMDs.....	34
9.3	CFD.....	35
9.3.1	Theory.....	35
9.3.2	Setup.....	38
9.4	CFD RESULTS.....	40
10	RESULTS.....	42
11	CONCLUSIONS.....	43
12	FUTURE WORK.....	44
13	BIBLIOGRAPHY.....	45
14	APPENDIX A - EQUATIONS.....	48
14.1	DENSITY - MIXTURE 2.....	48
14.2	DYNAMIC VISCOSITY - MIXTURE 2.....	48
14.3	COMBUSTION CHAMBER MASS FLOW RATE.....	48
14.4	EFFECTIVE EXHAUST VELOCITY.....	48
14.5	SPECIFIC IMPULSE.....	49
14.6	BOL PROPELLANT TANK PRESSURE.....	49
14.7	INJECTOR AREA.....	49
14.8	ΔV FOR HOHMANN TRANSFER.....	51
14.9	PROPELLANT MASS.....	52
14.10	PRESSURANT GAS WEIGHT.....	52
14.11	VANE WEIGHT.....	54
15	APPENDIX B - LMP-103S PROPELLANT VERIFICATION.....	55
15.1	MIXTURE PROPERTIES.....	55
15.2	COMBUSTION PROPERTIES.....	55
15.3	NASA CEA ANALYSIS.....	56

15.3.1 Program Results.....	56
15.3.2 R-Squared Determination.....	63

FIGURE 1: PROPOSED TIMELINE FOR THE 2014-2015 ACADEMIC YEAR.....	3
FIGURE 2: EQUIPMENT USED TO HANDLE HYDRAZINE.....	5
FIGURE 3: EQUIPMENT USED TO HANDLE LMP-103S.....	6
FIGURE 4: SHEAR STRAIN.....	12
FIGURE 5: LIQUID SIMULANT AND GEL SIMULANT WITH 5% CAB-O-SIL	13
FIGURE 6: ECAPS 1 N THRUSTER.....	15
FIGURE 7: SIMPLIFIED BLOWDOWN SYSTEM.....	16
FIGURE 8: TESTBED P&ID.....	19
FIGURE 9: PRESSURE TRANSDUCER OUTPUT VOLTAGE DIVIDER.....	20
FIGURE 10: TEST SETUP.....	21
FIGURE 11: LIQUID TESTBED RESULTS.....	21
FIGURE 12: LIQUID SCENARIO #1, #2 PRESSURE PLOTS.....	22
FIGURE 13: LIQUID SCENARIO #3.....	23
FIGURE 14: GEL TESTBED RESULTS.....	24
FIGURE 15: GEL SCENARIO #1.....	25
FIGURE 16: GEL WITH AIR POCKETS CLOGGING OUTLET.....	26
FIGURE 17: DOUBLET AND TRIPLET INJECTOR TYPES.....	27
FIGURE 18: TESTED PERFORMANCE AND CEA REPORTED PERFORMANCE VALUES FOR 1N THRUSTER	31
FIGURE 19: SIMPLE, PASSIVE SURFACE TENSION PMDS INSIDE SPHERICAL PROPELLANT TANK.....	33
FIGURE 20: SIMPLE VANE.....	34
FIGURE 21: CARREAU MODEL RELATIONSHIP.....	38
FIGURE 22: 13,000 CELL MESH.....	39
FIGURE 23: INITIAL VELOCITIES WITH VECTORS SHOWN WITH SURFACE TRACKING OF LIQUID AT 0.28 S AND GEL AT 0.01 S	40
FIGURE 24: LIQUID AND GEL MIXTURE AMOUNTS USING ACTUAL LMP-103S MASS PERCENTAGES. .	54
FIGURE 25: CEA GEL COMBUSTION VARIABLES.....	55

Nomenclature

<i>AA</i>	=	Ammonium Acetate
<i>ADN</i>	=	Ammonium Dinitramide
<i>CEA</i>	=	Chemical Equilibrium with Applications
<i>COTS</i>	=	Commercial off-the-shelf
<i>ECAPS</i>	=	Ecological Advanced Propulsion Systems
<i>HPGP</i>	=	High Propulsion Green Propellant
<i>LEO</i>	=	Low Earth Orbit
<i>NASA</i>	=	National Aeronautics and Space Administration
<i>O/F</i>	=	Oxidizer/Fuel ratio
<i>PMD</i>	=	Propellant Management Device
<i>PRISMA</i>	=	Prototype Research Instruments and Space Mission Advancement
<i>SCAPE</i>	=	Self-Contained Atmospheric Protection Ensembles
<i>SJSU</i>	=	San Jose State University

Symbols

A_c	=	feed line cross sectional area
A_{inj}	=	injector inlet cross-sectional area
A_t	=	throat area
c^*	=	characteristic exhaust velocity
cP	=	centipoise
d	=	diameter
g	=	gravity (9.81 m/s^2)
I_{sp}	=	specific impulse
K	=	Kelvin
k	=	head loss coefficient
kg	=	kilogram

L	=	length of graduated cylinder
\dot{m}	=	mass flow rate
N	=	number of injectors
μ	=	dynamic viscosity
P	=	pressure
Pa	=	Pascal
P_c	=	combustion chamber pressure
ΔP_{cool}	=	pressure loss due to regenerative cooling
ΔP_{dyn}	=	pressure loss due to dynamic pressure
ΔP_{feed}	=	pressure loss due to feed lines
ΔP_{inj}	=	pressure loss due to injector
P_T	=	propellant tank pressure
r	=	<i>radius</i>
ρ	=	density
R_G	=	pressurant gas constant
s	=	seconds
T_c	=	combustion chamber adiabatic flame temperature
T_G	=	pressurant gas mean temperature
ν	=	kinematic viscosity
v_{inj}	=	flow velocity through injector
V_T	=	propellant tank volume
W_G	=	pressurant gas weight in propellant tank

1 Introduction

Space continues to be the up and coming frontier for exploration and technological advances. All areas of space development will depend on spacecraft propulsion. Different missions will require different propulsion methods. Small satellites have recently become more popular as the importance of worldly data collection grows. An efficient, reliable, and safe propulsion method is needed now to supply small satellite missions for consumers such as Skybox Imaging, a Google acquired satellite company that aims to operate a constellation of earth imaging spacecraft in low earth orbit.

The monopropellant hydrazine was and continues to be a popular fuel used to maneuver spacecraft. It is well known that hydrazine has good performance characteristics but is plagued with safety liabilities such as toxicity, hazardous and costly operational handling, and harmful environmental impact (Larsson & Wingborg, 2011). Recent efforts are concentrated to create a high performance green propellant (HPGP) to replace and improve hydrazine in those regards.

The highly effective monopropellant LMP-103S consisting of ammonium dinitramide (ADN), methanol, ammonia, and water is a tried and tested HPGP that helps to solve the shortcomings of hydrazine while increasing performance characteristics by 30% and reducing mission costs. The technology has been developed by Ecological Advanced Propulsion Systems, ECAPS, in association with the Swedish Space Corporation and is currently and successfully being flight-tested onboard both PRISMA satellites.

Skybox Imaging currently has plans to use this ADN based monopropellant in liquid form for future satellites. Liquid monopropellants, however, introduce required propellant management devices to deal with slosh and controlled fuel placement within the propellant tank.

2 Motivation

There is increasing interest from the military and space organization to use thixotropic fuels to improve propellant performance and simplify propellant systems while increasing handling safety and reliability.

Skybox Imaging is attracted to the prospect that pseudoplastics could minimize or eliminate slosh and propellant management devices (PMDs) all together, decreasing initial hardware costs and launch weight. PMDs may come in the form of bladders, pistons, diaphragms, or bellows that physically separate the propellant and pressurant gas. If slosh is not left as an unknown variable, the placement of fuel could be accurately known within the propellant tank and therefore make the delivery of the propellant to the tank outlet very reliable.

3 Project Objective and Requirements

This research project will focus on testing and validating a gelled version of LMP-103S to incorporate into future Skybox satellite generations. The idea is that a gelled propellant will eliminate the need for PMDs and provide the same flight characteristics as the liquid monopropellant while being safer to handle and therefore reducing costs.

Requirement for the project:

1. The new propellant and a potentially new propulsion system are required to fit within the current satellite housing dimensions of 60cm x 60cm x 16cm
2. Provide similar I_{sp} as the liquid propellant, $\pm 5\%$
3. The propulsion system must be able to expel at least 90% of the gel propellant
4. The gel propellant must be able to flow predictably and reliably
5. The propellant system must deliver gas-free propellant to the feed lines

4 Project Timeline

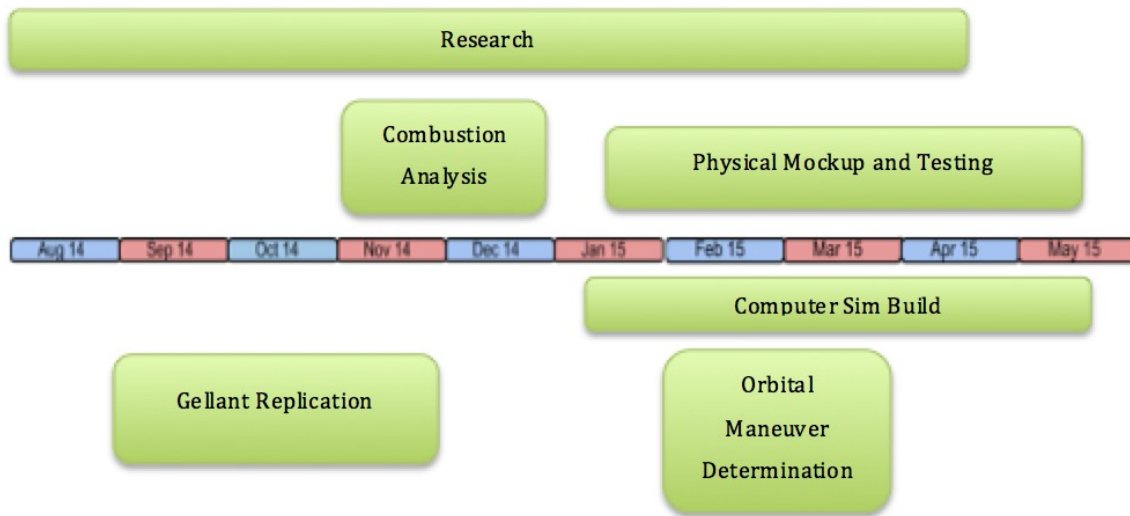


Figure 1: Proposed timeline for the 2014-2015 academic year

5 Literature Overview

Satellite propulsion for spacecraft in low earth orbit (LEO, 160 – 2000 km above the Earth’s surface) is a means to counteract gravity and the forces encountered in the thin atmosphere. In order for a satellite to complete its objectives, it has to follow the pre-planned trajectory defining the mission. Orbital stationkeeping is the use of propulsion to make these slight changes to correct the spacecraft’s trajectory and to

stay aligned with the mission profile. On small satellites orbiting the Earth, thrusters can be used to achieve stationkeeping.

The monopropellant hydrazine, first used in WWII by the Germans to create the first rocket-powered fighter jet, is the most commonly used fuel used in the space environment for thrust and landing purposes. Hydrazine provides thrust by interacting with a catalyst that causes the liquid propellant to expand exothermically. The hot gases are expelled through the thruster in one direction, pushing the satellite in the opposite direction. Hydrazine's properties and performance capabilities are well known which is why it is still in use today. A recent and well-known example is the descent stage rocket propellant used by NASA's Curiosity rover.

Hydrazine, however, is very toxic and dangerous to manipulate. Handling requires special equipment and can be very costly to transport (Beckel & Dinardi). It is estimated that the transportation and disposal of hydrazine costs ~ \$29/lb. Storage and monitoring of hydrazine can grow that cost to more than three times that amount (Dinardi, 2013). It also requires the launch facility to put Self-Contained Atmospheric Protection Ensembles (SCAPE) into place.

The cost of working with and disposing of hydrazine created a need to develop a new type of monopropellant. Ammonium dinitramide based propellants were presented as a viable option to reduce handling costs while providing the same, if not better, on orbit performance.



Figure 2: Equipment used to handle hydrazine (Beckel & Dinardi)

The Zelinsky Institute in Moscow and the Stanford Research Institute in the U.S. were the first organizations to recognize the potential of ADN, a high-energy inorganic salt oxidizer. It was recognized that it easily dissolved in polar solvents such as water which led to its development as an oxidizer in liquid propellants while a solid propellant option was also researched as a possibility (Larsson & Wingborg, 2011).

Two ADN-based liquid propellants, LMP-103S and FLP-106, were developed further because of their thermally stable qualities (directly relatable to a long storage lifetime) and performance characteristics. The goal was to create monopropellants that were comparable to hydrazine but without the handling dangers. When compared side by side, FLP-106 shows better performance characteristic than LMP-103S.

Performance Property	FLP-106	LMP-103S
I_{sp} (s)	259	252
ρ (g/cm ³)	1.362	1.240
$\rho^* I_{sp}$ (gs/cm ³)	353	312

Table 1: Propellant performance properties (Larsson & Wingborg, 2011)

ECAPS focused their efforts to test and evaluate LMP-103S as a potential candidate to replace hydrazine. They found that normal personal protective equipment such as gloves and goggles and other low level personal protective equipment were sufficient to handle the monopropellant. The chemical subcomponents are biodegradable, it is able to be transported via air, land, and sea, and can be stored for more than twenty years in contact with COTS equipment when kept within its operating temperature. These reductions in safety requirements create lower costs and allows for a very tight and rigid ground schedules regarding launch preparations.

Comparing figures of merit of hydrazine to LMP-103S, the HPGP has a 24% higher density, 6% higher specific impulse, lower freezing point, and is stable. These factors make LMP-103S a highly acclaimed propellant to replace hydrazine.

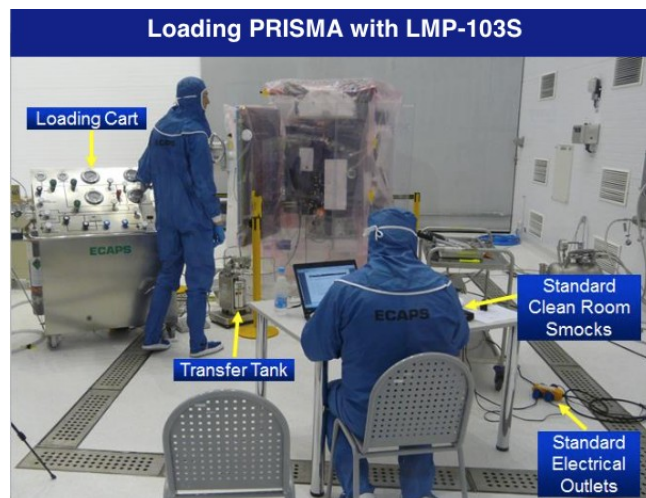


Figure 3: Equipment used to handle LMP-103S (Beckel & Dinardi)

In addition, LMP-103S was verified to meet the European Space Agency's quality requirements when hot fired with 1 N thrusters (Neff, King, Anflo, & Möllerberg, 2009). 1 N thrusters were used when the monopropellant was flight tested successfully aboard the PRISMA

Mango satellites, the same size thrusters that Skybox Imaging will be using on their satellites.

The combination of less costly handling equipment, less propellant (because of its efficiency) which leads to smaller tanks and less waste, and lower transportation costs leads to a more inexpensive option to hydrazine. Although initial thruster and propellant costs for LMP-103S are higher, these will decrease as the technology matures and production volume increases. Though the clean up costs of LMP-103S are comparable to hydrazine (~ \$29/lb), excess HPGP may be disposed of in an open burn (Dinardi, 2013).

5.1 LMP-103S

Skybox Imaging chose the LMP-103S monopropellant because of the previously mentioned characteristics. The propellant also provides enough ΔV to perform required maintenance maneuvers including drag makeup, orbital phasing within the constellation, and possible altitude lowering and raising.

For the sake of this project, only LMP-103S will be tested and considered as a viable propellant to be used in future Skybox Imaging satellites. ECAPS and Skybox are familiar with its performance characteristics. If those characteristics do not change significantly when gelled, it will be easier to integrate this propellant rather than FLP-106, another HPGP propellant that may or may not be compatible with the systems currently in place for LMP-103S.

The rocket fuel hydrazine has been used since World War II and is commonly used for space attitude control so its properties and performance parameters are well known. There are however many

drawbacks to using this toxic propellant as mentioned above. It will only be used as a baseline to measure against the performance of LMP-103S.

The chemical structure of the propellant is as follows (mass percentages): 60-65% ADN, 15-20% methanol, 3-6% ammonia, and the remaining water. Additional properties are listed below.

Property	Hydrazine	LMP-103S
Specific Impulse* (s)	220	235
Density @ 25°C (kg/m ³)	1003.7	1240 (24% higher than hydrazine)
Specific Heat (J/ (kg·K))	3077.8	2420
Thermal Expansion Coefficient (1/K)	9.538E10-4	N/A
T _{chamber} (K)	1666	~1881
Freezing point (K)	275	183
Melting point (K)	274.54	267
Boiling point (K)	387	393
Operating temperature range (K)	283-323	283-323 (allows use of COTS hydrazine components)
Viscosity (cP, mPa·s)	0.913	3.3m – 3m
Blow down ratio*	4:1	4:1
Cold start capability	No	No
Toxicity	High	Low
Storable	Yes	Yes (> 6.5 yrs)
Corrosive	Yes	No
Sensitive to air or humidity exposure	Yes	No
Exhaust Species	NH ₃ , N ₂ , H ₂	H ₂ O (50%), N ₂ (23%), H ₂ (16%), CO (6%), CO ₂ (5%)
Stability	Up to 422 K	Stable > 20 yrs (STANAG 4582)
Handling Hazards	Toxic, flammable	Environmentally benign

Table 2: Propellant properties measured at 25°C

* 1 N thruster performance

(Neff, King, Anflo, & Möllerberg, 2009) (Beckel & Dinardi) (Huzel & Huang, 1967)
(Huzel & Huang, 1967)

6 Methodology

To test if a gelled monopropellant is a viable replacement for the liquid propellant, three different test scenarios will be attempted. One will be a physical modeling of a simplified propellant system, including a simulated propellant for which the flow properties will be obtained. Another scenario pertains to combustion that will be dealt with computationally using NASA's Chemical Equilibrium with Applications program. The last test will utilize computational fluid dynamics to validate the zero gravity characteristics of the fluid in the propellant tank using ESI's computational fluid dynamics program CFD-ACE+.

7 Physical Modeling and Testbed

7.1 LMP-103S Simulant

It is expensive, hard to obtain, and dangerous to work with LMP-103S propellant for testing purposes. Therefore a liquid will be created to simulate LMP-103S in order to test the physical fluid flow throughout the propellant system. Once the liquid is found to be a suitable simulant, it will be turned into a gel.

Chemical Compound	Molecular Formula	Weight Percentage (%)
ADN	$\text{NH}_4\text{N}(\text{NO}_2)_2$	65-60
Methanol	CH_3OH	20-15
Ammonia	NH_3	6-3
Water	H_2O	Balance

Table 3: LMP-103S chemical composition

The simulant must be safe to handle during the testing phase. Once the solution is created, tests will be performed to compare viscosity,

density, and surface tension between the solution and known physical chemical properties of LMP-103S.

7.1.1 Simulant Selection

The ADN oxidizer component will be replaced by readily obtainable ammonium acetate (AA). AA has a slightly lower melting point at 114°C and can harmlessly decompose in ammonia and water (Linde, 2012). It is possible to dissolve the same amount of AA in water as ADN, even though ADN has a higher solubility. The simulant will be created with help from the San Jose State University's Randy Kirchner with the College of Science providing the materials, chemicals, and lab space.

7.1.2 Liquid Simulant Creation

The liquid solution will be created using the mass percentages for LMP-103S shown below. For testing and validation purposes, one liter of solution will be produced.

Chemical Compound	Molecular Formula	Mass Percentage Mixture 1	Mass Percentage Mixture 2	Mass Percentage Mixture 3
Ammonium Acetate	$C_2H_3O_2NH_4$	53.5	48	50
Methanol	CH_3OH	26.5	19.5	23
Ammonia	NH_3	6.5	4	5
Water	H_2O	13.5	28.5	22

Table 4: Liquid simulant composition (Linde, 2012)

The correct amounts of ammonium acetate and distilled water are first added to a container followed by the more volatile chemicals methanol and ammonia. The ammonium acetate starts to dissolve when the

water and methanol are introduced and were left in the sealed container to thoroughly mix and warm back up to room temperature.

Three different mixtures were created and tested to obtain a solution that had mimicked properties similar to the actual LMP-103S propellant. Mixture 2 had the closest matching physical properties and will be used to test the fluid flow in the physical testbed.

7.1.3 Simulant Testing and Validation

Density and viscosity were two properties tested to validate the LMP-103S liquid simulant. Surface tension was measured and will be referenced when researching propellant management devices using CFD in the tank redesign. A size 200 Cannon-Fenske viscometer and a No. 70535 tensiometer with a 70537 platinum ring were used to measure viscosity and surface tension, respectively, and a graduated cylinder and scale for density.

Once the simulant was found to have comparable properties (listed in Appendix B) to the actual propellant, a thickener was mixed in to observe how the propellant would perform as a gel.

7.1.4 Gel Simulant

7.1.4.1 *Thixotropy*

A gel is said to be thixotropic if the fluid's viscosity decreases with an increasing shear strain rate. Shear strain is a function of deformation, or more specifically, shear deformation and is measured in radians. It helps to describe the strain using the figure below.

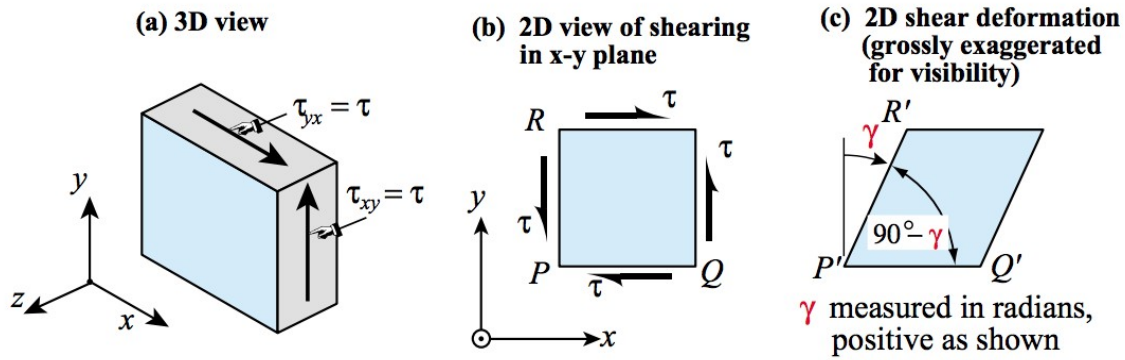


Figure 4: Shear strain
(University of Colorado Boulder)

When a shear stress $\tau_{xy} = \tau_{yx}$ is applied along the face of the element, the element is deformed. This creates a new angle between the sides PR and PQ. The change in this angle expresses the shear strain the element undergoes.

A good example of applying a shear stress to a thixotropic fluid would be squeezing a plastic ketchup container and forcing the ketchup to move and flow out of the container. In this case it can be imagined that there are infinitesimally thin parallel layers sliding against each other in the same direction. Strain rate is measured by the displacement of each layer as a function of its distance from a fixed wall (y).

$$\dot{\epsilon} = \frac{\partial V}{\partial y}(y, t) \quad (1)$$

$V(y, t)$ is the parallel velocity of a layer measured at a distance y from a fixed wall. The shear strain for a non-Newtonian fluid can be described using the Power Law also known as the Ostwald-de Waele relationship seen below.

$$\mu_{eff} = K \left(\frac{\partial u}{\partial y} \right)^{n-1} \quad (2)$$

The effective viscosity, μ_{eff} , is characterized by the flow consistency index K , the shear rate, and the dimensionless flow behavior index n . For this case, $n < 1$ to represent a pseudoplastic. A Newtonian fluid has a value of 1 for n .

7.1.5 Gel Simulant Creation

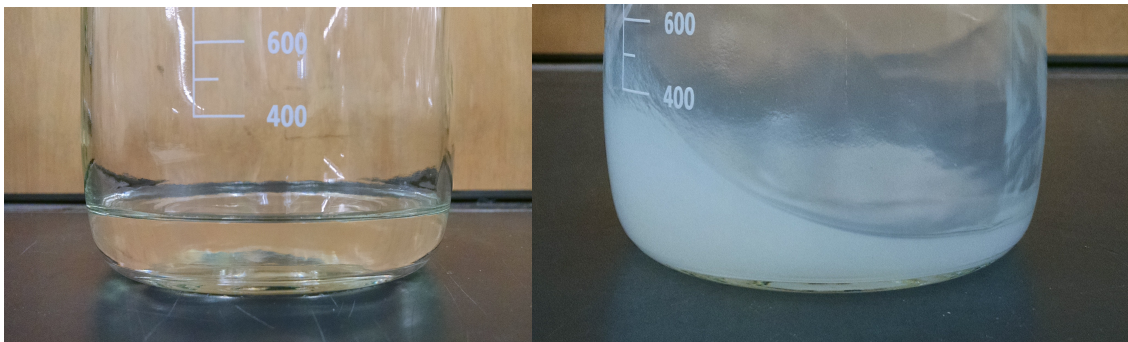


Figure 5: Liquid simulant (left) and gel simulant with 5% Cab-O-Sil (right)

Adding Cab-O-Sil to the liquid simulant will create the gel. Cab-O-Sil is superfine fumed silica (SiO_2) that, when added to a liquid, increases thixotropic properties as well as viscosity without significantly increasing density (Product Bulletin 14, 2013), all of which are desirable for this project's propellant. It was found that adding 4% of the fumed silica by weight created the targeted gel. Density, viscosity, and surface tension measurements were taken again for the gel, shown below in Table 5.

The viscosity of the gel however was much more difficult to measure with a viscometer and was approximated by filling a graduated cylinder with the gel simulant and dropping a sphere of known density and diameter into it, timing its travel between two designated points.

It is interesting to note that for solid propellant based on ADN, Cab-O-Sil is added to the prilled oxidizer to prevent caking of the material

(Larsson & Wingborg, 2011). Firing tests performed by Intech with this solid propellant show that it is already possible to mix in the fumed silica to create a viable rocket propellant.

Property	LMP-103S	Liquid Simulant	Gel Simulant 4% Cab-O-Sil by weight
Density (kg/m ³)	1240	1019.06	1071.11
Dynamic Viscosity (Pa·s)*	0.0033 - 0.003	0.00513	16.75 ⁺
Kinematic Viscosity (cSt)*	2.66-2.42	4.872	15637.98
Surface Tension (N/m)	0.0373	0.040	0.0700

Table 5: Simulant properties for Mixture 2
 * 20 - 25°C
 + (Green, Rapp, & Roncace, 1991)

For the case of a real propellant and not one for test purposes, small aluminum particles can be added to a monopropellant to create a thixotropic gel. The additive increases density and density impulse.

7.2 Gel Disadvantages

When the gel is forcefully sloshed in its container a thin layer coats the walls. This residual will remain on the container walls, separated from the propellant bulk mass near the tank outlet until a sufficient enough shearing force is applied to get the fluid moving again. The residual quantity will be higher for gels than liquids, enough to where it should be compensated (larger tank, more propellant).

Small decreases in specific impulse have also been seen in the past. . This is possible because the thixotropic agent dilutes the propellant. Also, injectors are not able to effectively atomize the incoming

propellant in certain cases, affecting the overall O/F ratio and burn efficiency.

Again, the purpose this experiment is to gel the LMP-103S in such a way that by the time the monopropellant reaches the injector it will have reacquire it's liquid properties so this will not pose a problem and to see how much of the performance is affected. This project will take into account residual propellant left in the tank but injector atomization efficiency is left as a point for further research.

7.3 Propellant System

7.3.1 Thruster Performance

The driving mechanism behind the properties that will define the propellant system is the thruster. The first iteration of Skybox propulsion satellites will use 1 N thrusters. The optimal combustion parameters using the flight proven 1 N thrusters will be used to determine the necessary fluid flow properties entering the combustion chamber. From there the pressure within the propellant tank and the types of PMDs, if necessary, can be determined.

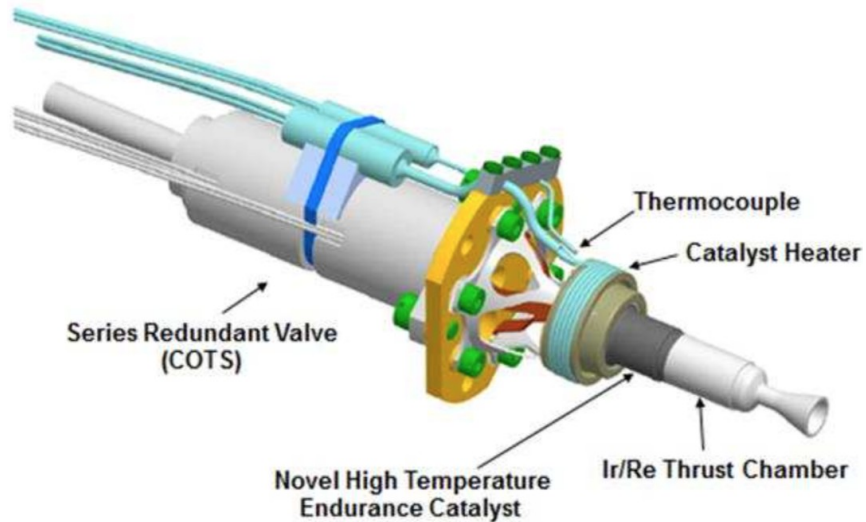
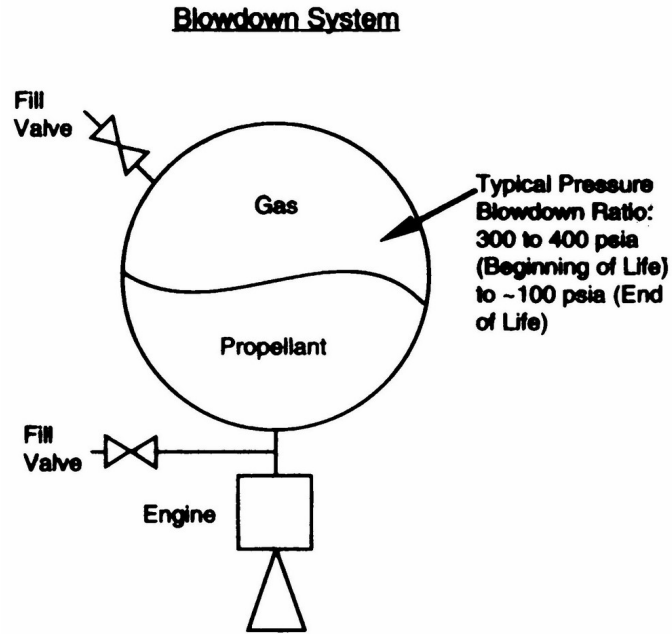


Figure 6: ECAPS 1 N thruster (Dinardi, 2013)

7.3.2 Pressure Levels

The BOL pressure value is very important to the overall performance of the propulsion system. In a typical blowdown system, such as used in Skybox Imaging's satellites, an inert pressurant gas (helium, nitrogen, hydrogen, or oxygen) is stored inside the propellant tank along with the propellant. This gas pushes the propellant through the feed lines to the combustion chamber of the thrusters. The pressure in the tank determines the chamber pressure and thus the specific impulse and thrust performance.



**Figure 7: Simplified blowdown system
(Liquid rocket systems)**

The analysis starts with the chamber pressure to make sure the engine is reaching the required performance levels necessary for the mission. From there the pressure drops in the feed system are accounted for and the BOL pressure of the pressurant gas in the propellant tanks can be acquired.

7.3.3 BOL/EOL Propellant Tank Pressure

Pressure losses throughout the system are inevitable to it is important to characterize the necessary chamber pressures to define the initial tank pressure. Pressure losses are associated with dynamic pressure $\Delta P_{dynamic}$, pressure drop ΔP_{feed} in the feed system, pressure drops from the cooling jacket in regenerative cooling systems ΔP_{cool} , and the pressure drop introduced in the injector ΔP_{inj} . ΔP_{cool} can be ignored in this case since radiation cooling is used in place of regenerative cooling.

The BOL pressure is the sum of the chamber pressure and pressure losses.

$$P_{tank, BOL} = P_c + \Delta P_{dynamic} + \Delta P_{feed} + \Delta P_{inj} \quad (3)$$

where

$$\Delta P_{dynamic} = \frac{1}{2} \rho_i V^2 \quad (4)$$

$$\Delta P_{feed} = 50000 \text{ Pa (conservative)} \quad (5)$$

$$\Delta P_{inj} = 0.2 P_c \text{ (unthrottled)} \quad (6)$$

This BOL pressure helps define the blowdown ratio, or the ratio between the BOL and EOL pressure. The maximum BOL and minimum EOL chamber pressure according to ECAPS is 2200000 Pa and 550000 Pa, respectively (Sjoberg, Skifs, Thormahlen, & Anflo, 2009). Therefore the blowdown ratio for the ECAPS propellant system is 4. The mass flow rate drops from 4.34E-4 kg/s producing 1 N of thrust at BOL to 1.34E-4 kg/s at EOL to provide 0.27 N.

7.3.4 Pressurant Gas

The gas that is pressurizing the propellant tank and pushing the propellant to the combustion chamber is delicately matched with the monopropellant, tank environment, and tank geometry. In addition the gas must not be soluble in the propellant or be able to condense to avoid additional pressure losses. The actual gas used to pressurize LMP-103S tanks is helium and will be used for testing purposes. The calculations below use gaseous helium as the acting pressurant gas.

The required pressurant weight in the tank W_g is calculated by the following equation.

$$W_g = \frac{P_T V_T}{R_g T_g} \quad (7)$$

where P_T is the propellant tank pressure, V_T the empty tank volume, R_g the pressurant gas constant, and T_g the mean temperature of the gas. The calculation is found in Appendix A where W_g for helium is found to be 0.0309 kg to provide a ΔV of 219 m/s.

The propellant and pressurant mass is scaled down for the testbed run. One 0.0005 m³ (0.5 L) tank is used. For the tank pressure to start at 2.2E6 Pa and have an EOL pressure of 5.5E5 Pa, there needs to be an initial amount of 0.3883 kg of gel simulant in the tank at BOL. Of the 0.5 L, the gaseous helium will fill 0.1375 L.

7.3.5 Throat Area and Mass Flow Rate

ECAPS has designed the 1 N thrusters that will be used on the satellites Skybox will be sending into LEO. The goal of this Master's project is to design the adjusted gel propellant system to adhere to the current thrusters and the existing combustion chamber properties.

The specific impulse obtained from optimal combustion conditions with a 1N thruster is 235 s. The mass flow rate needed to produce the chamber pressure is determined by the following formula (Humble, Henry, & Larson, 1995).

$$\dot{m} = \frac{T}{I_{sp} g_o} = 4.34E-4 \frac{kg}{s} = 0.434 \frac{g}{s} \quad (8)$$

The throat cross-sectional area A_t of the nozzle can be found with the proceeding equation

$$A_t = \frac{\dot{m} c^i}{P_c} = 4.05E-4 m^2 \quad (9)$$

7.4 Propellant System Testbed

The validation portion of this project consists of building a physical propellant system and analyzing the fluid flow from the propellant tank to the end of the feed line.

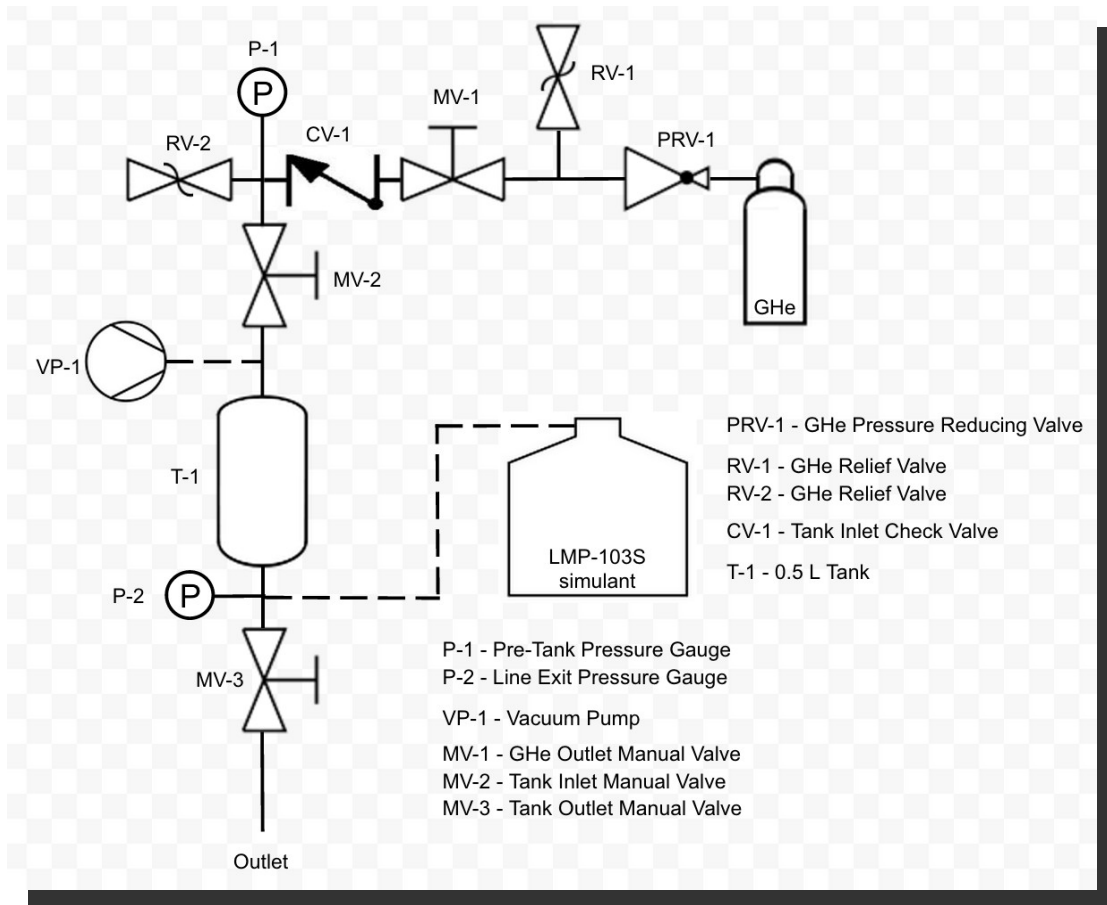


Figure 8: Testbed P&ID

Before any simulant is introduced, the propellant system testbed is weighed and the dry mass obtained. The liquid simulant is first loaded into the propellant tank by a vacuum pressure applied on the opposite side of the tank. Gaseous helium then pressurizes the tank to $2E6$ Pa. The second manual valve is opened and measurements of flow velocity and pressure of the fluid are taken at the end of the feed line. The pressure transducer's 10V output is led to a voltage divider as seen in Figure 9 so the Arduino UNO can read the entire voltage (5V max). The measurement values are passed to a computer where they can be

plotted in real-time. The mass is recorded as well to calculate the mass flow rate of the ejecting propellant. This process is repeated with the gel simulant. This will test if the gel is able to re-obtain its liquid properties at the end of the feed line.

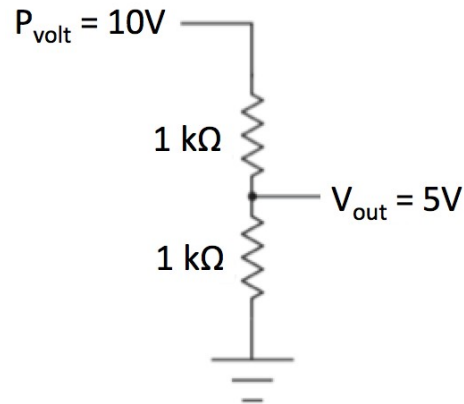


Figure 9: Pressure transducer output voltage divider

Three scenarios will be looked at to compare the liquid and gel flow characteristics.

1. Feed line commissioning (first 3 seconds) - Initial state does not have any propellant in the feed line. MV-2 is opened and measurements and total propellant throughput is measured until steady state pressure measurements are read from the Arduino.
2. Steady state (until 100 psi) - Initial state has the feed line filled with propellant. MV-2 is opened and measurements and total propellant throughput is measured well into the steady state time period.
3. End of life (100 psi to ~ 70 psi) - Initial state has the feed line filled with propellant. MV-2 is opened and measurements and total propellant throughput is measured until all usable propellant has exited the feed line.

A testbed stand was built to hold the propulsion module and to allow for a catch tank at the outlet. The ejected simulant is weighed after each scenario to determine the mass flow rates for each regime. After

all three scenarios are done and all helium escapes, the propellant testbed is weighed again. The increase in mass denotes the trapped propellant mass left in the tank at EOL. Unfortunately, a quickly pulsed-thrust scenario cannot be tested due to a lack of materials and will be left for future analyses.

An AIAA grant set up by Abhra Dasgupta and a donation by Skybox Imaging provided the funds for all the materials.

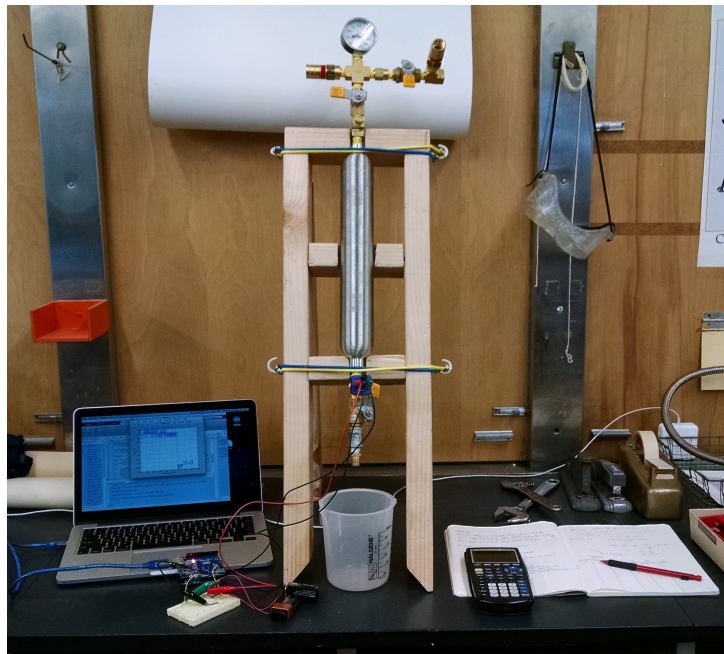


Figure 10: Test setup

7.5 Testbed Results

7.5.1 Liquid

To end up with an EOL pressure of $5.5E5$ Pa for a 0.5 L tank, 0.3625 L of the liquid simulant (0.3694 kg) is filled into the tank. $2E6$ Pa of helium then pressurizes the system. The results for the three combustion scenarios are below (see Appendix A).

Scenario	P_{start} (Pa)	P_{end} (Pa)	\dot{m} (g/s)	Time (s)
1	1,625,783	1,487,888	5.30	3.00*
2	1,487,888	697,060	3.81	55.46
3	697,060	568,955	3.03	26.64

Figure 11: Liquid testbed results
* Experimental flaw

The mass flow rates presented above are roughly an order of magnitude higher than what is expected with the real propulsion system. This is due to the limitation of the orifice size (0.04064 cm used for all tests) available commercially. The mass flow rate at BOL was higher but this is correlated with the inability to stop the flow exactly after 3 seconds. The BOL pressure was also lower than the ideal 2E6 Pa because of complications getting the flow to exit smoothly initially.

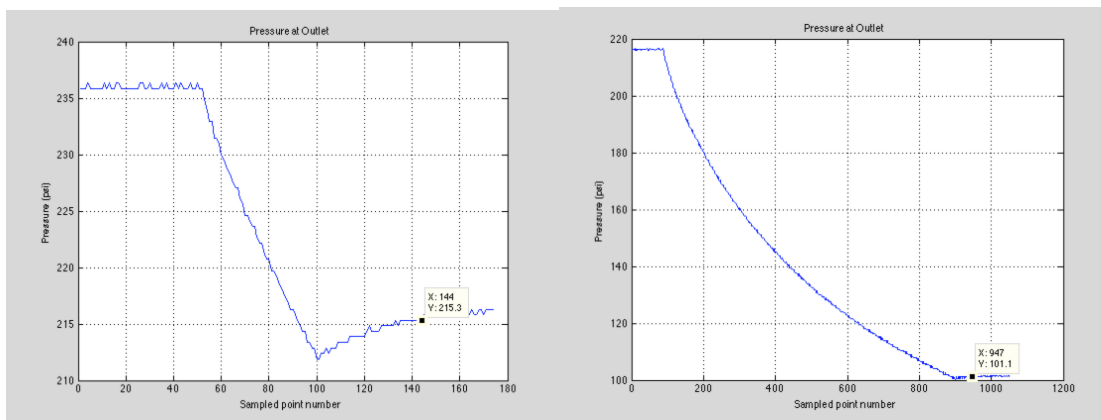


Figure 12: Liquid scenario #1 (left), #2 (right) pressure plots

The above plots show the pressure trends as time increases. Testbed commissioning sees a linear (slight exponential) pressure drop for the first scenario and an exponentially decreasing trend for the steady state. An exponential trend is expected because this is a blowdown system and the gaseous helium pressurant is filling the area left by the exiting simulant. The exponential trend is also experienced at EOL scenario #3.

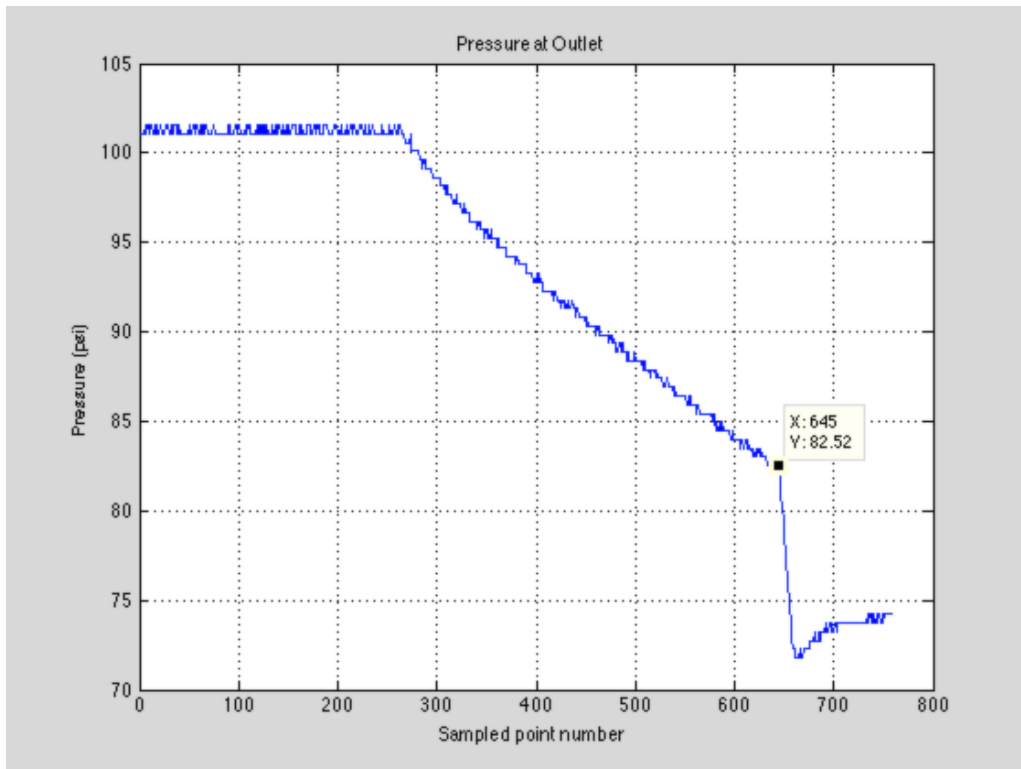


Figure 13: Liquid scenario #3

The sharp decrease in pressure shows that there is no more simulant in the tank to push out and so the helium escapes. The last simulant escapes with the tank holding a pressure of 82.52 psi, or 568,817 Pa, which is right above the expected EOL tank pressure.

Only a 0.3 gram increase was seen when the testbed was weighed again after the helium was expelled. For this case with a 0.3 g propellant residual, there is a 99.92% expulsion efficiency. These results are expected overall for the liquid simulant.

The liquid came out with a blue-ish tint in the catch tank. The density was measured again and saw a 2.64% increase, leading to the assumption that the helium was dissolving in the simulant.

7.5.2 Gel

The gel test required 0.3625 L or 388.3 g to be loaded into the tank and then pressurized. The commissioning scenario went smoothly and started at the BOL pressure of 2E6 Pa.

Scenario	P _{start} (Pa)	P _{end} (Pa)	\dot{m} (g/s)	Time (s)
1	2,073,943	1,895,369	2.19	3.52

Figure 14: Gel testbed results

The mass flow rate was significantly slower for the gel. This shows that the gel simulant is not regaining its liquid physical properties and/or is not traveling through the orifice effectively. The plot below shows that some helium left the outlet before the gel was able to. This is a problem because combustion instability can occur if the gel sets into a solid-like state with helium trapped within it and sent to the injector.

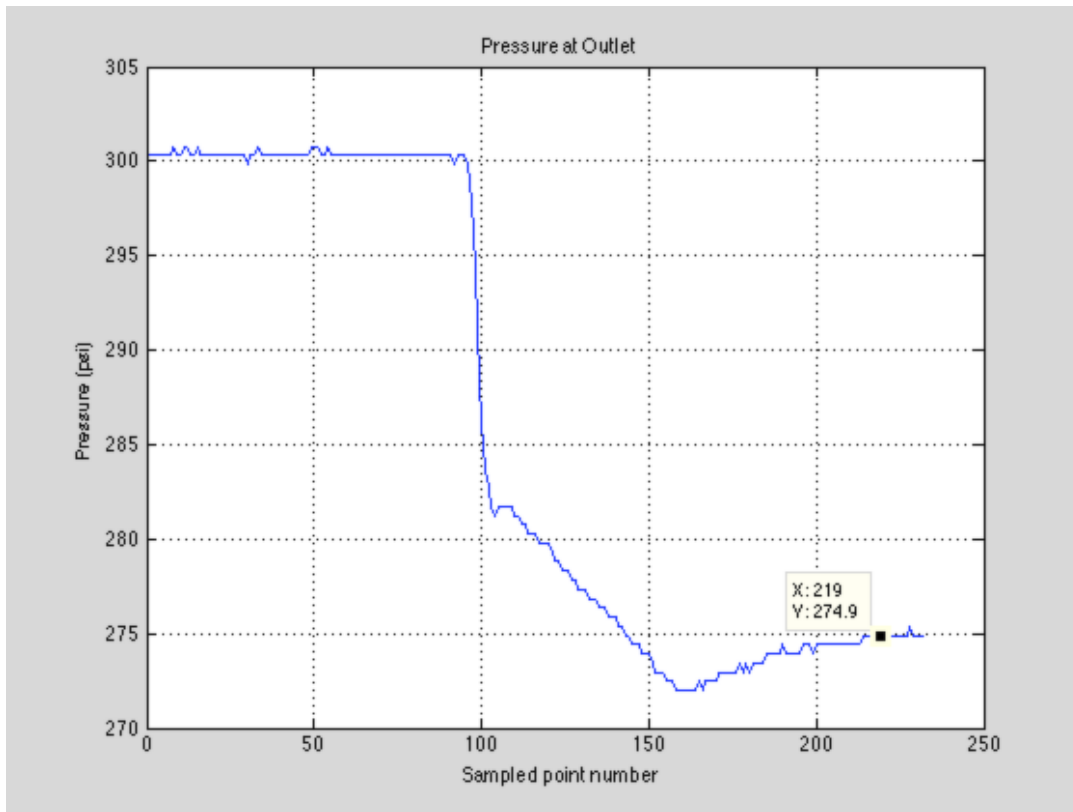


Figure 15: Gel scenario #1

The gel presented more complications during the other scenarios. When BV-2 was opened for the steady state test, the orifice outlet sputtered and then emitting propellant. Everything passed BV-2 was cleaned and a steady stream of simulant was seen before the flow halted. The same results were experienced several times after the downstream parts were clean repeatedly. During the sporadic flows, which lasted around 30 seconds, the same exponential pressure trend could be seen on the real-time plot with the mass flow rates averaging 1.10 g/s. The inconsistency in the flow however only allowed the pressure to drop to 1,255,535 Pa, well above the EOL pressure.

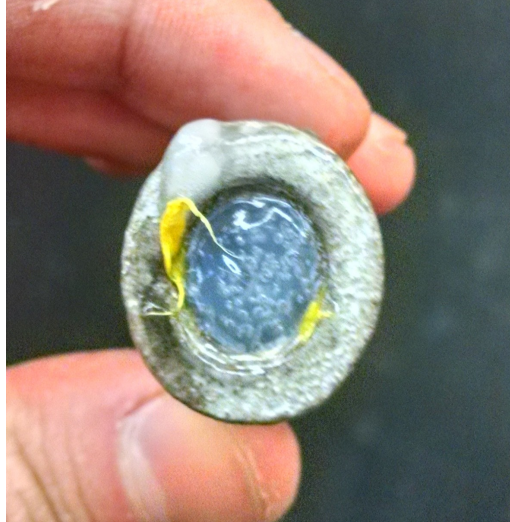


Figure 16: Gel with air pockets clogging outlet

It was thought that there needed to be more pressure in the tank since the BOL test worked, so the pressure was brought back up to $2E6$ Pa. Still nothing left the outlet.

Overall, the gel tests presented a slower moving fluid that was filled with air pockets and clogged the outlet. Unfortunately this consequence does not lead to the amount of residual propellant left in the tank, and any mass savings/gains that result from that.

7.5.2.1 *Injector Analysis*

The orifice (injector) is the limiting factor in the gel expulsion tests. It is very difficult to design an injector because so many parameters need to be optimized such as the number of orifices, impingement angles, flow rates, combustion stability, etc. It becomes a simpler analysis if the parameters are analyzed separately, or are decoupled from each other.

Atomization is a main concern for gel propellants because the surface tension forces are much higher than the inertial forces of the high velocity fluid. Once the gellant is through the orifice it needs to be

atomized efficiently in order to burn efficiently and wholly. Smaller droplets and gel relaxation times characterize atomization quality.

Better atomization results can be seen using doublet (self-impinging) or triplet injector types. The injectors here cause the propellant streams to impinge, which promote intimate mixing and good atomization. Although these techniques are typically referenced when mixing fuels and oxidizers, the same concept can be applied with the gel monopropellant.

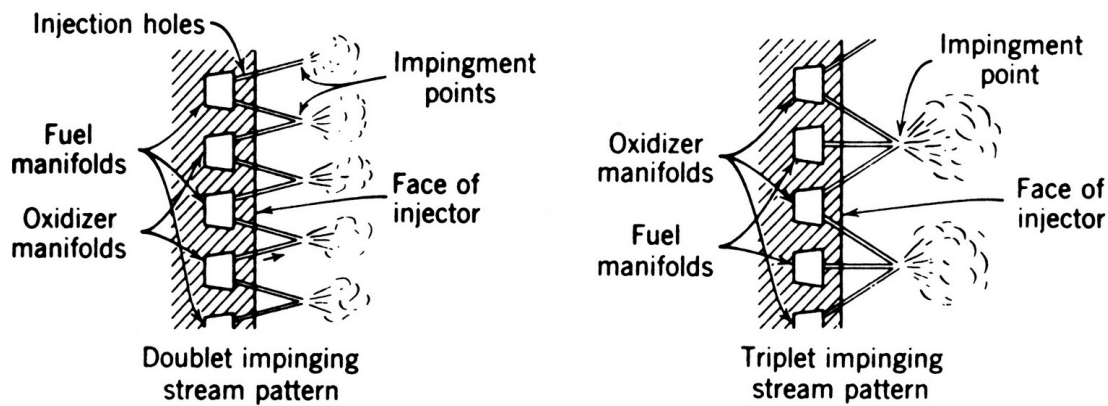


Figure 17: Doublet and triplet injector types (Huzel & Huang, 1967)

The equations describing the physical injector attributes are

$$A_{inj} = \frac{\dot{m}}{N} \sqrt{\frac{K}{2\rho\Delta P_{inj}}} \quad (10)$$

$$v_{inj} = \frac{\dot{m}}{A_{inj} N \rho} \quad (11)$$

A_{inj} = injector inlet cross-sectional area

N = number of injectors

k = head loss coefficient (1.2 for radiused inlet, 1.7 for nonradiused)

v_{inj} = flow velocity through injector

The equation implies that as the number of flow channels increases, the mass flow rate and the area per injector decrease. Smaller droplet atomize better with small injector area that also mean higher propellant velocities entering the combustion chamber (Humble, Henry, & Larson, 1995).

A 1991 NASA study containing a water-gel formulation with similar properties to the LMP-103S simulant published that atomization improves when mass flow rate increases (Green, Rapp, & Roncace, 1991). High mass flow rates correspond with high Reynolds number where the inertial forces dominate over viscous forces. Visually, this agrees with a uniform spray of small droplets. The gel simulants that were tested however experience the opposite, which delays the onset of turbulent flow, inhibiting quality atomization. If the mass flow rates were lessened and a self-impinging injector stream was utilized it could be possible to still see quality atomization at lower flow velocities.

Another approach would be to look at adding 3.5% of the Cab-O-Sil thickener by weight to the liquid simulant rather than the 4% studied here. 3.5% showed good thixotropic properties and the gel would flow more freely with less shear strain applied. This would be the next step in the testing phase, however the lack of chemicals inhibited this testing.

This is left for future investigation because any calculations made here would extend beyond the scope of this project. The techniques provided in (Huzel & Huang, 1967) and (Sutton & Biblarz, 2001) can be used as design guides.

7.5.2.2 Viscosity and Heaters

The gel is considered a thixotropic fluid meaning that it is a non-Newtonian fluid and its viscosity is time dependent. The fluid will coalesce into a more liquid state if a shear thinning strain is applied at a constant rate. Heat may also be added to lower the viscosity of the liquid, making it a temperature dependent viscous fluid as well.

Active thermal control systems such as cartridge heaters could be used to heat the gel within the tank where patch heaters would encompass the feed lines to keep the temperature of the fluid constant to the injector. This would help the gel obtain higher mass flow rates when the valves are initially open.

8 Combustion

8.1 Chemical Equilibrium with Applications

NASA's Chemical Equilibrium with Applications program is used to determine the chemical equilibrium composition of complex reactions and the output performance parameters for various applications (McBride & Gordon, Computer Program for Calculation of Complex Chemical Equilibrium Compositions and Applications, 1996). Liquid LMP-103S is first run with CEA and combusted to make sure the results are comparable to known, published values. Afterwards the gel LMP-103S propellant is simulated and compared to the liquid results.

8.2 Combustion Simulation and Analysis

The NASA computer program CEA (McBride & Gordon, Chemical Equilibrium with Applications, 2010) is used to determine the combustion characteristics of the liquid propellant and make sure that they line up appropriately with published data. This helps to prove the

validity of the program for the experiment at hand. This legitimacy test also refines the programmable inputs that are used to get them as accurate as possible through iteration. After CEA proves to be valid and the appropriate inputs are defined, the gelled version of LMP-103S will be simulated and the properties obtained.

CEA is used to compute the characteristic velocity, specific impulse, and other useful parameters of combustion for LMP-103S given the adiabatic flame temperature (1881 K), combustion chamber pressure (2E6 Pa), and other chemical properties. The knowledge gained here will help find the necessary properties of the propulsion systems upstream of the combustion chamber (e.g. pressure losses and propellant BOL pressure in tank).

8.2.1 Combustion of Liquid LMP-103S

Below are the input properties used to simulate the combustion of the liquid monopropellant.

		Molecular Formula	ΔH_f° (kJ/mol) *	Incoming temperature to combustion chamber (K)	Combustion Temperature ⁺ (K)
Fuel	Methanol	CH ₃ OH	-238.6	308	1881
	Ammonia	NH ₃	-80.8	239	1881
Oxidizer	Water	H ₂ O	-285.8	308	1881
	ADN	NH ₄ N(NO ₂) ₂	134.6	308	1881

Table 6: LMP-103S combustion properties. Cab-O-Sil only used for gel combustion
* Liquid reactants

⁺ Combustion temperature based on ADN (Dinardi, 2013)

A typical propellant tank pressure for a liquid monopropellant blowdown propulsion system is $2E6$ Pa (Liquid rocket systems) on the low end. From here the backed-out chamber pressure P_c is found to be $1.573E6$ Pa resulting in an I_{sp} of 228 seconds using the CEA program setup seen in Appendix B. This calculation was done for all chamber pressures used in the plot below.

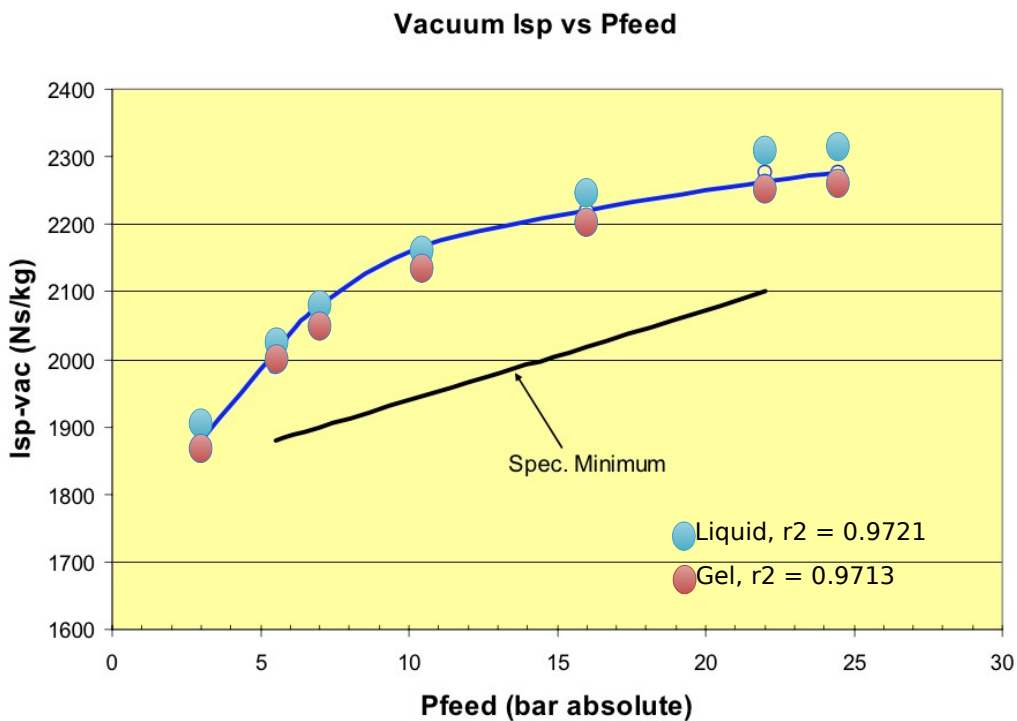


Figure 18: Tested performance and CEA reported performance values for 1N thruster (Moore, Anflo, & King, 2009)

The blue line in the figure above is the ECAPS published and flight verified I_{sp} values. The overlaid blue data points are the I_{sp} values reported at given combustion chamber pressures after running the CEA program at the designated pressure for the liquid propellant, and the red points for the gel. The residuals, or r^2 values, for both the liquid and gel CEA simulated propellants are random and is an acceptable figure and CEA will be used to examine the combustion of the gel propellant.

8.2.2 Combustion of Gel LMP-103S

The liquid propellant was modified in the CEA program by adding in the thickener silica quartz (SiO_2) as an oxidizer. This changed the mass percentages of the oxidizers and fuels, seen in Appendix B. The new O/F ratio is 3.04 with the addition of 4.96 g (4% by mass) Cab-O-Sil. The results showed, as expected, that the specific impulse values were slightly lower than the liquid combustion. This is attributed to the silica diluting the liquid monopropellant. The average percentage change between the liquid and gel I_{sp} is -1.65%. This fulfills the project-imposed requirement that the gel propellant must provide similar I_{sp} as the liquid propellant, $\pm 5\%$.

8.3 Combustion Results

Figure 18 above shows a direct comparison to the liquid and gel CEA combustion and experimentally obtained data. Because the starting max I_{sp} is 231s for the gel (4s lower than published liquid results), we would need to carry an extra 0.1814 kg (1.8% increase) of propellant and 0.0006 kg of helium pressurant (1.9% increase) to make up for the lower I_{sp} . The tank volume also increases by 0.0001 m^3 (1.1% increase) to compensate for the extra tank cargo, an overall 0.1820 kg.

It is important to note that these results apply to the used propellant during its lifetime and do not take into account the residual gel left in the tank. Unfortunately the experiments using the physical testbed were unable to provide EOL residual propellant left in the tank. This residual needs to be accounted for when calculating the amount of usable propellant sufficient for the mission.

9 Propellant Management Devices

9.1 Slosh

Slosh is the behavior and movement of the propellant when the tank is jostled due to spacecraft accelerations. The objectives of PMDs are to reliably store and position the propellant in its tank and to deliver gas-free propellant to the combustion chamber in a reduced gravity environment, helping to cancel out the effects of slosh. Positive PMDs employ physical barriers for separation between the pressurant gas and propellant where passive PMDs rely on surface tension to keep the propellant in contact with the propellant drain (Humble, Henry, & Larson, 1995).

9.2 Elimination of PMDs

A goal of using a gel propellant is to eliminate the need for PMD devices. The phases of a satellite's mission that introduce slosh and uncertainty regarding the propellant's placement within the holding tanks are the launch/boost phase, detumbling, and slewing maneuvers. Complex PMDs are required depending on the possible orientations of the propellant during stages of the mission.

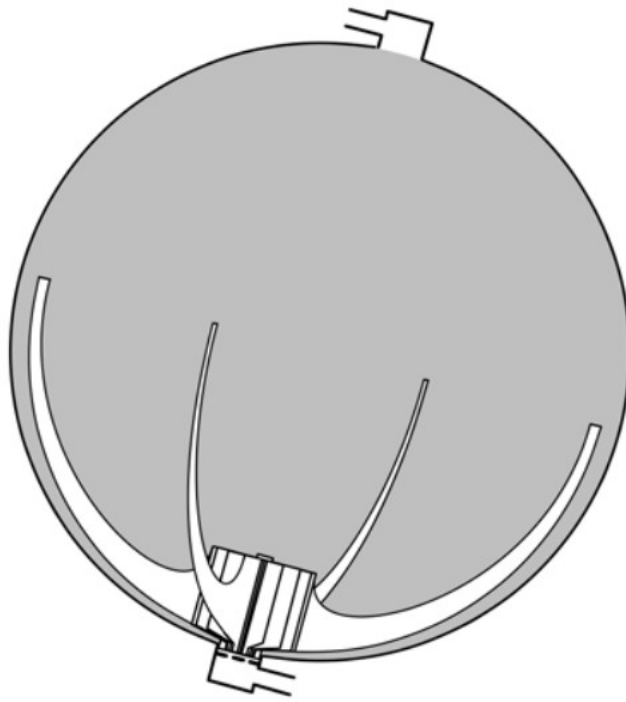
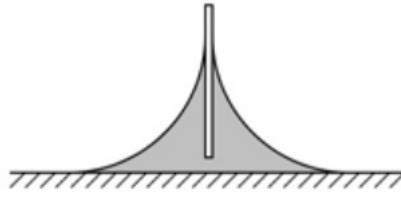


Figure 19: Simple, passive surface tension PMDs inside spherical propellant tank (Jaekle, Jr, 1991)

The gel propellant is more viscous, which increases the internal friction of the fluid and a resistance to shearing flows. The gel naturally does not slosh as much as a more inviscid fluid meaning it can be compartmentalized to one area. The theory is that the gel can be localized around the tank outlet at all times without using any PMDs, even simple, non-complex porous plates and vanes. Porous plates and sponges act as surface tension devices and could further help to localize and maintain propellant around the outlet. Vanes passively apply a driving pressure to overcome hydrostatic pressure to move to the outlet. This pressure difference is driven by surface tension.



**Figure 20: Simple Vane
(Jaekle, Jr, 1991)**

Issues may arise when the pressurized gas is in contact with the gel propellant. It is possible for the gas to dissolve in the propellant, which would change the density and reduce the specific impulse of the monopropellant and the pressure within the tank (Sutton & Biblarz, 2001), affecting the performance of the thrusters. A density increase of 5.1% was seen when the physical model was tested. A diaphragm PMD would avoid gas-propellant contact but is ignored for this experiment.

9.3 CFD

9.3.1 Theory

The overarching governing Navier-Stokes equations that describe the flow of a fluid are well known to aerospace engineers. Computational fluid dynamics programs analyze these equations using a flow model that assumes fluid moving through an infinitesimal fluid element fixed in space. This flow model requires the differential equations to conserve mass, momentum, and energy.

$$\text{Global Continuity: } \frac{\partial \rho}{\partial t} + \nabla \cdot (\rho \vec{V}) = 0 \quad (12)$$

$$\text{Conservation of Momentum: } \frac{\partial (\rho u)}{\partial t} + \nabla \cdot (\rho u \vec{V}) = -\frac{\partial p}{\partial x} + \rho f_x$$

$$\text{Conservation of Momentum: } \frac{\partial (\rho v)}{\partial t} + \nabla \cdot (\rho v \vec{V}) = -\frac{\partial p}{\partial y} + \rho f_y$$

$$\text{Conservation of Momentum: } \frac{\partial(\rho w)}{\partial t} + \nabla \cdot (\rho w \vec{V}) = -\frac{\partial p}{\partial z} + \rho f_z \quad (13)$$

$$\text{Conservation of Energy: } \frac{\partial}{\partial t} \left[\rho \left(e + \frac{V^2}{2} \right) + \nabla \cdot \rho \left(e + \frac{V^2}{2} \right) \vec{V} \right] = \rho \dot{q} - \frac{\partial(\rho u)}{\partial x} - \frac{\partial(\rho v)}{\partial y} - \frac{\partial(\rho w)}{\partial z} + \rho \vec{f} \cdot \vec{V} \quad (14)$$

The physics of slosh can be described by the governing incompressible Euler equations seen below (Hunter, 2006).

$$\frac{\partial \vec{u}}{\partial t} + \vec{u} \cdot \nabla \vec{u} + \nabla p = 0 \quad (15)$$

$$\nabla \cdot \vec{u} = 0 \quad (16)$$

Equation (15) shows that a fluid particle's acceleration is proportional to the pressure force enacted upon it. The nonlinear advection term $\vec{u} \cdot \nabla \vec{u}$ makes this a nonlinear partial differential equation and inherently difficult to solve. Numerical methods and linearization are used to approximate the nonlinear solutions. Computational fluid dynamics is an example of numerical method applications. CFD can solve full Navier-Stokes (continuity, momentum, and energy) equations without further geometrical or physical simplifications. The nonlinearity is solved for at discrete points which form a grid in the computer model.

The second equation introduces the incompressible condition meaning density remains constant (density is set equal to 1 in the first equation). To analyze the free surface motion of the gel, the velocity potential (17) is substituted into Equation (16) to give Equation (18).

$$\vec{U} = \nabla \phi \quad (17)$$

$$\nabla^2 \phi = 0 \quad (18)$$

Equation (18) is Laplace's Equation and by solving for the velocity potential ϕ with given boundary conditions, all properties for an irrotational, isentropic flow can be calculated.

Viscosity is an important variable and plays a role in the slosh analysis for this project. We look to the incompressible Navier-Stokes equation to fulfill this requirement.

$$\frac{\partial \vec{u}}{\partial t} + \vec{u} \cdot \nabla \vec{u} + \nabla p = \nu \Delta u \quad (19)$$

Above, ν is the kinematic viscosity. All the equations shown here form the basis for the CFD scenario that will test the effectiveness of the gel propellant to reduce or fully eliminate slosh.

The CFD-ACE+ software tracks the fluid interface by computing the volume fraction (a single scalar field variable, F) of one of the immiscible fluids in each computational cell. For example, in this case, ACE+ is tracking gaseous helium and gelled LMP-103S. If F has a value of 1, the cell is filled only with helium. If F has a value of 0, the cell is filled only with gelled LMP-103S. A fraction means both fluids occupy that cell. From this the fluid-fluid boundary can be tracked using a Piecewise-Linear Interface Calculation.

Surface tension is also included in the free surface model. Surface tension, when surrounded by the same species, is zero because the net force of the surrounding molecules pulling on the central molecule, which pulls back, cancels out. However, the surface molecules are not surrounded by as many like molecules as in the bulk of the species and therefore cohere more strongly with the other surface molecules, resulting in a nonzero force per unit length. In ACE+, it is seen as a net normal force acting on the surface. Viscosity is accounted for using the Power Law described above.

The physics behind PMDs can be described by capillary action, which is influenced by the pressure difference ΔP at the interface of two immiscible fluids, surface tension γ , and the radii of curvature R_1 and

R_2 for an arbitrarily curved surface (National Programme on Technology Enhanced Learning).

$$\Delta P = \gamma \left(\frac{1}{R_1} + \frac{1}{R_2} \right) \quad (20)$$

$$\Delta P = \gamma \left(\frac{z_x}{x(1+z_x^2)^2} + \frac{z_{xx}}{(1+z_x^2)^{\frac{3}{2}}} \right) \quad (21)$$

Equation (21) is the general PDE form of Equation (20) (the subscript x demonstrates the partial derivative of z with respect to x). Passive PMDs rely on this wicking force to remain near the tank outlet to provide gas-free propellant to the combustion chamber.

9.3.2 Setup

SolidWorks is first used to create the propellant tank part. Propellant sloshing is the only concern for analysis here so only the tank is modeled, meaning no feed lines are attached at the outlet. The CFD programs used in this analysis are CFD-GEOM and CFD-ACE+, both products of the ESI Group. The three-dimensional part and structured mesh were created in CFD-GEOM. CFD-ACE+, the flow simulator, is a multi-physics and multi-disciplinary simulation tool. Its built-in volume of fluid free surface module can be applied to the immiscible fluid-sloshing problem to solve the incompressible, viscous fluid flow Navier-Stokes equations. The transient time dependent option is selected to track the volume fraction of a species in each cell to determine which fluids are present, tracing the movement of the flow. In the time dependent case run here, another algorithm in CFD-ACE+ calculates the volume fraction in a cell from one time step to the next. The proportions of the fluids in the mixture determine the physical properties present in a given computational cell.

LMP-103S properties were input into the liquid database in CFD-ACE+ for the respective liquid and gel models. The surface tension of the gel simulant (0.07 N/m) was used in place of the program default value. The density of the LMP-103S gel was assumed to increase by 6.5% from the liquid value (average increase for gel simulant) to 1321 kg/m³.

The liquid viscosity was modeled on piecewise linear relation for temperature because the viscosity of liquid LMP-103S is temperature dependent. A total of 11 tabulated values allow the solver to interpolate or extrapolate values as needed. The Carreau Law is the viscosity model for the gel which and accounts for the shear rate. Viscosity based on temperature is unknown for the gel so that property was not a variable used in the Carreau Law, which is seen below.

$$\mu = \mu_{\infty} + (\mu_0 - \mu_{\infty}) \left[1 + (K \dot{\gamma}^a)^{\frac{n-1}{a}} \right]^{-1} \quad (22)$$

μ is the effective dynamic viscosity value at the given shear rate, μ_{∞} the viscosity at infinite shear rate, μ_0 the viscosity at zero shear rate, λ the relaxation time constant, $\dot{\gamma}$ the shear rate, n the Power Law index where $n < 1$ signifies a pseudoplastic, and a the ratio of activation energy to thermodynamic constant. The relationship of viscosity and shear rate for the Carreau model shows that the effective viscosity decreases as shear rate increases (ESI-Group, 2014).

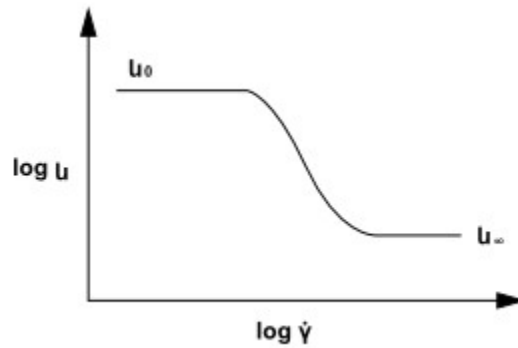


Figure 21: Carreau model relationship

Since the LMP-103S gel simulant viscometer measured an apparent infinite number, a viscosity of 16.75 Pa·s was pulled from the NASA study (Green, Rapp, & Roncace, 1991) and used since the rheological properties with the water-gel mixture were comparable.

Both the liquid and gel simulations were run in zero-gravity environments with an initial condition angular velocity of 15°/s to simulate a tumbling satellite coming off the launch vehicle at a high angular rate which is the most the satellite will experience during its mission lifetime. The cylinder geometry is meshed with 13,000 cells. A grid independence study was performed with double and triple the amount of cells, which agreed with the results produced by the original mesh.

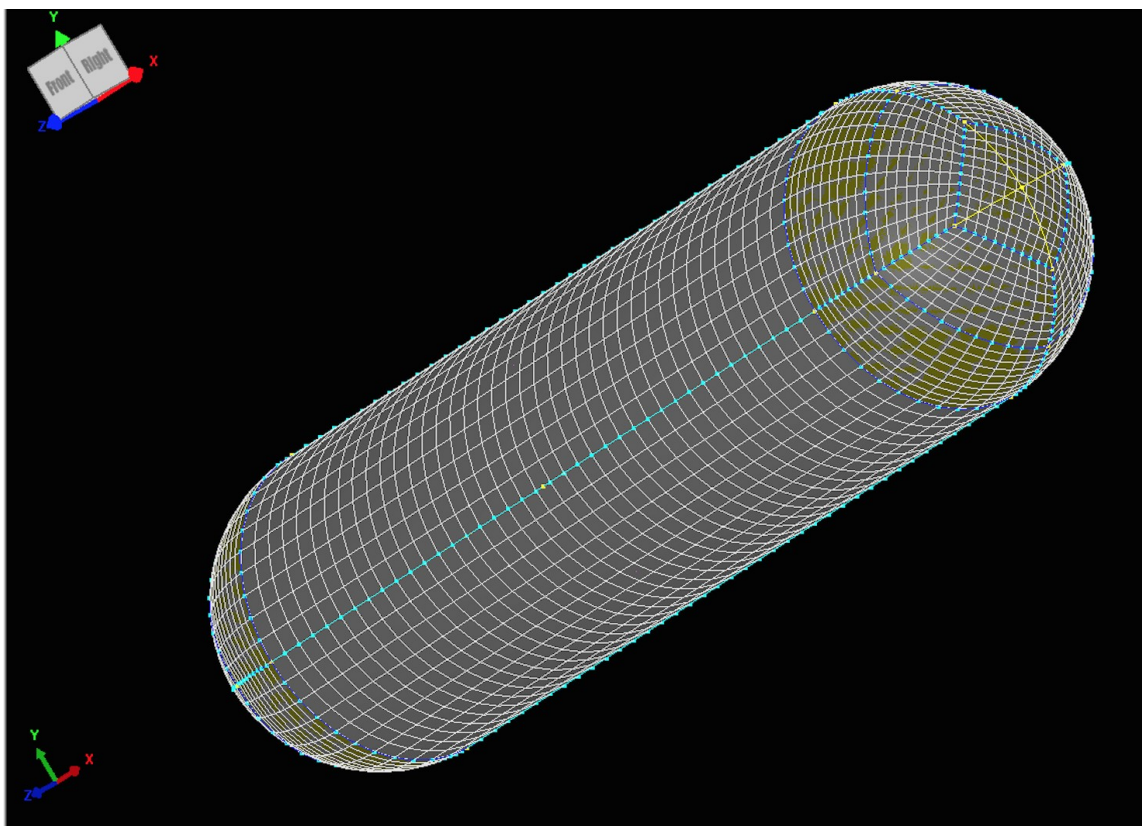


Figure 22: 13,000 cell mesh

9.4 CFD Results

The ACE+ solver shows that, for the liquid LMP-103S near EOL, the fluid sloshes and climbs up the side of the tank with the applied initial condition. The simulation shows that the liquid movement and placement is not reliable enough, without PMDs, to deliver gas-free propellant to the nozzle combustion chamber.

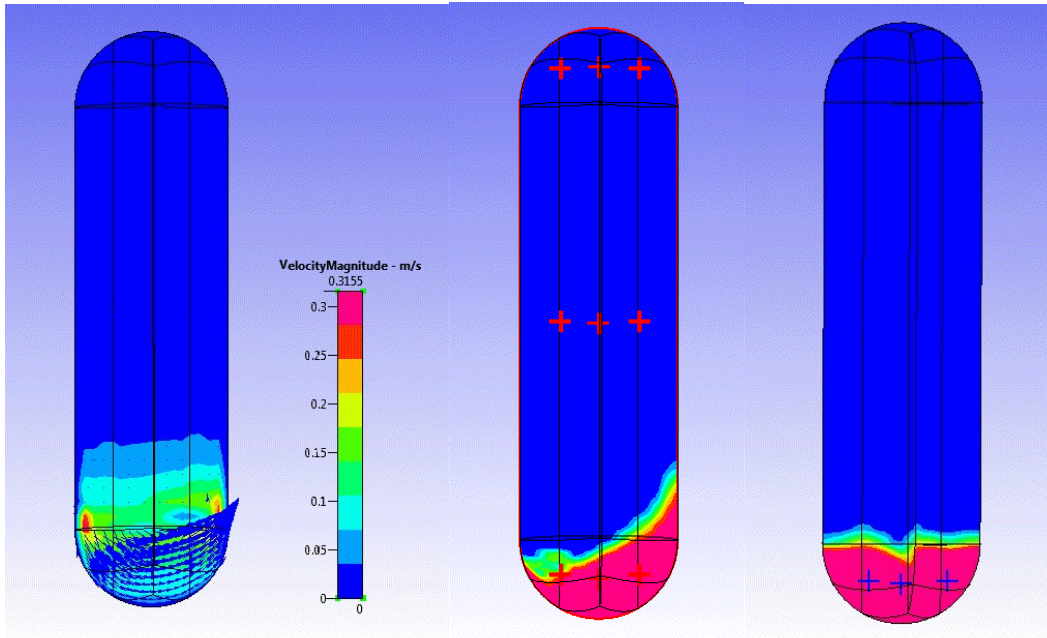


Figure 23: Initial velocities with vectors shown (left) with surface tracking of liquid at 0.28 s (middle) and gel at 0.01 s (right)

Figure 23 shows the general tendencies of the tested fluids when the same initial angular velocities are applied. The liquid is inclined to climb up the side of the wall because its inherent viscous forces are not enough to overcome the applied external force. The liquid surface shows that its positioning is fully dependent on applied external forces, validating it would need propellant tank PMDs to keep the fluid from moving away from the tank outlet. However, the gel's non-Newtonian structure resists the initial acceleration, leaving the surface contact points at the tank walls relatively stable. The center of the gel surface sloshes slightly which dissipates the added energy caused by the angular rate.

The gel simulation shows that the initial condition does not have an effect on the propellant placement. It is apparent that the rapid $15^\circ/\text{s}$ jolt (occurs solely in the first timestep) is not high enough to overcome the zero shear rate viscosity $\mu_0 = 16.75 \text{ Pa}\cdot\text{s}$. From this simulation, the

gel validates the theory that it does not need any PMDs to control its placement in the propellant tank.

A CFD grid dependency study shows there is no dependence on the grid used for simulations. Meshes with 25,704 and 38,804 cells, double and triple the cell count from the initial mesh, support the results here.

10 Results

Data gathered from the testbed analysis were inconclusive but some insight can be drawn from the results. First is that the gel introduces slower mass flow rates to the existing propellant system. This will lead to lower quality atomization using the current injector and possibly less efficient fuel burn in the combustion chamber. A higher propellant throughput could help to solve these problems and requires more testing. Residual propellant left in the propellant tanks at EOL could not be calculated. That number would have led to the overall mass savings/addition to the current propulsion system.

Combustion data from CEA shows that the gel performance is lower than the liquid I_{sp} by 1.65%. This requires the satellite to hold 0.1820 kg more propulsion to compensate for the performance drop. Residual propellant left in the tank would require more initial propellant as well, however it is deemed to be small, though not insignificant.

Simulation results from CFD visually show that PMDs can be removed from the propellant tank based on the initial angular velocity of $15^\circ/s$ applied in the first time step. The resultant average strain rate of 0.05 s^{-1} reported by ACE+ is not high enough to advance the thixotropic gel's position within the tank. If PMD usage were kept to a minimum

(four simple vanes) for the liquid propellant, the total PMD mass would be 1.37 kg. The space freed up by removing PMDs would allow for 0.2248 kg more gel propellant to be carried. To make up for the I_{sp} mass losses, the potential extra propellant mass comes to 0.0428 kg.

Combining the mass gains from the I_{sp} and losses from eliminating PMDs results in a net loss of 1.19 kg from the current the propellant system.

11 Conclusions

This project demonstrated that a gelled version of LMP-103S is feasible.

The project requirements are stated here again to reiterate the goals of this experiment.

1. The new propellant and a potentially new propulsion system are required to fit within the current satellite housing dimensions of 60cm x 60cm x 16cm
2. Provide similar I_{sp} as the liquid propellant, $\pm 5\%$
3. The propulsion system must be able to expel 90% of the gel propellant
4. Gel propellant must be able to flow predictably and reliably
5. The propellant system must deliver gas-free propellant to the feed lines

Combustion simulation with NASA's CEA program demonstrated it is possible to gel the liquid monopropellant with little loss of specific impulse, losing only a small amount of its initial I_{sp} , but still satisfies requirement (2). Requirement (1) is met because the tank and feed system dimensions have not changed. The testbed showed that the

current injector would have to be modified to accommodate the gel's flow properties to uphold requirement (4) and was inconclusive on the expulsion percentage needed to evaluate requirement (3). The CFD results show the thixotropic gel's viscosity is able to keep the gel at a fixed position over the tank outlet, allowing for gas-free propellant delivery to the combustion chamber proving the feasibility of requirement (5). Slosh is not a factor and therefore PMDs controlling slosh can be eliminated from the design. The overall propellant system weight is also reduced, decreasing overall costs.

Overall I believe the tank modifications, weight savings, and possible changes to the injector are feasible design goals for the Skybox Imaging satellites. The new tank design simplifies manufacturing and increases the amount of propellant can be carried. The injector alterations, if necessary, will prove to be more difficult to carry out.

12 Future Work

Given more funding, future work can focus further on viscosity and the affects of fluid flow when heaters and temperature fluctuations are introduced. It has only been speculated in this report that an increase in temperature would benefit injector atomization.

This project fell short testing the physical fluid flow of the gel. The very next step would be to create and study a gel with 3.5% thickener added to the liquid simulant rather than 4%, which was analyzed here. The 3.5% gel simulant would behave more like a liquid and would need less applied shear strain to get it moving initially. This change could solve the injector issues. Only the 4% case was looked at here because the amount of ammonium acetate was limited.

If the 3.5% still presented the fluid flow problem seen with the 4%, testing may benefit from a new injector design to first allow the gel to flow out of the testbed and second to atomize the fluid thoroughly upon exit. Characterizing the exit conditions will allow for tweaking of the internal conditions so that combustor performance is optimized.

13 Bibliography

- 1) Beckel, S., & Dinardi, A. *High-Performance Green Propulsion (HPGP) for Improved Performance, Responsiveness and Reduced Lifecycle Cost*. Presentation, Space Tech Expo: Satellite Space Summit.
- 2) Dinardi, A. (2013, March). High Performance Green Propulsion (HPGP) - On-Orbit Validation and Ongoing Development.
- 3) ESI-Group. (2014, July). CFD-ACE+ V2014.0: Modules Manual, Part 1. Huntsville, AL, USA: ESI-Group.
- 4) Green, J. M., Rapp, D. C., & Roncace, J. (1991). *Flow Visualization of a Rocket Injector Spray Using Gelled Propellant Simulants*. Sverdrup Technology, Inc. Brook Park: NASA Lewis Research Center.
- 5) Humble, R. W., Henry, G. N., & Larson, W. J. (1995). *Space Propulsion Analysis and Design* (First - REVISED ed.). (R. W. Humble, G. N. Henry, & W. J. Larson, Eds.) New York: The McGraw-Hill Companies, Inc.
- 6) Hunter, J. K. (2006). *An Introduction to the Incompressible Euler Equations*. UC Davis, Department of Mathematics.
- 7) Huzel, D. K., & Huang, D. H. (1967). *Design of Liquid Propellant Rocket Engines*. Washington, D.C.: National Aeronautics and Space Division.
- 8) Jaekle, Jr, D. E. (1991). *Propellant Management Device Conceptual Design and Analysis: Vanes*. PMD Technology. Lafayette: AIAA.
- 9) Larsson, A., & Wingborg, N. (2011). Green Propellants Based on Ammonium Dinitramide (ADN). *InTech* , 139-156.
- 10) Linde, R. (2012). *Liquid Monopropellant Injector Development for High Power Electrodes Plasma Thruster*. KTH

School of Electrical Engineering, Space and Plasma Physics
Department. Stockholm: KTH.

- 11) *Liquid rocket systems*. (n.d.). Retrieved 10 24, 2014, from Delft University of Technology: <http://www.lr.tudelft.nl/index.php?id=26229&L=1>
- 12) McBride, B. J., & Gordon, S. (2010, 03). *Chemical Equilibrium with Applications*. (D. J. Zehe, Editor, & National Aeronautics and Space Administration) Retrieved 11 2014, from Glenn Research Center: <https://cearun.grc.nasa.gov/>
- 13) McBride, B. J., & Gordon, S. (1996). *Computer Program for Calculation of Complex Chemical Equilibrium Compositions and Applications*. Cleveland: NASA.
- 14) Moore, S., Anflo, K., & King, P. (2009). *Expanding the ADN-Based Monopropellant Thruster Family*. ECAPS, ATK Tactical Propulsion & Controls, and Moog Inc. AIAA.
- 15) National Programme on Technology Enhanced Learning. (n.d.). *Laplace Pressure and Young-Laplace Equation*. Retrieved from NPTEL: <http://nptel.ac.in/courses/103105065/M6I6.pdf>
- 16) Neff, K., King, P., Anflo, K., & Möllerberg, R. (2009). High Performance Green Propellant for Satellite Applications. *AIAA* , 1-13.
- 17) *Product Bulletin 14*. (2013). Retrieved September 5, 2014, from TAP Plastics: http://www.tapplastics.com/uploads/pdf/Product_Bulletin_14-2013.pdf
- 18) Shchetkovskiy, A., McKechnie, T., & Mustaikis, S. (2012, August 13). Advanced Monopropellants Combustion Chambers and Monolithic Catalyst for Small Satellite Propulsion. (P. Processes, Compiler) Huntsville, AL.
- 19) Sjöberg, P., Skifs, H., Thormahlen, P., & Anflo, K. (2009). *A Stable Liquid Mono-Propellant based on ADN*. Insensitive

- Munitions and Energetic Materials Technology Symposium,
Tuscon.
- 20) Sutton, G. P., & Biblarz, O. (2001). *Rocket Propulsion Elements* (7th ed.). New York: John Wiley & Sons.
 - 21) Tam, W., Ballinger, I., & Jaekle, D. (2008). *Propellant Tank with Surface Tension PMD for Tight Center-of-Mass Propellant Control*. ATK Space. American Institute of Aeronautics & Astronautics.
 - 22) *The Individual and Universal Gas Constant*. (n.d.). Retrieved Dec 6, 2014, from The Engineering ToolBox:
http://www.engineeringtoolbox.com/individual-universal-gas-constant-d_588.html
 - 23) University of Colorado Boulder. (n.d.). *Introduction to Aerospace Structures*. Retrieved 03 30, 2015, from
<http://www.colorado.edu/engineering/CAS/courses.d/Structures.d/IAST.Lect04.d/IAST.Lect04.pdf>

14 Appendix A - Equations

14.1 Density - Mixture 2

Liquid Simulant

$$\rho = \frac{m}{V} = \frac{0.0101906 \text{ kg}}{0.010 \text{ m}^3} = 1019.06 \frac{\text{kg}}{\text{m}^3} \quad (23)$$

Gel Simulant

$$\rho = \frac{m}{V} = \frac{0.0107111 \text{ kg}}{0.010 \text{ m}^3} = 1071.11 \frac{\text{kg}}{\text{m}^3} \quad (24)$$

14.2 Dynamic Viscosity - Mixture 2

Liquid Simulant

Kinematic Viscosity

$$\nu = (\text{efflux time})(\text{viscometer constant}) = (48.72 \text{ s})(0.1) = 4.872 \text{ cSt} \quad (25)$$

Cannon-Fenske size 200 viscometer constant = 0.1

Dynamic Viscosity

$$\mu = \nu \rho = (4.872 \text{ cSt}) \left(1052.8 \frac{\text{kg}}{\text{m}^3} \right) = .00513 \text{ Pa} \cdot \text{s} \quad (26)$$

14.3 Combustion chamber mass flow rate

$$\dot{m} = \frac{T}{I_{sp} g_o} = \frac{1 \text{ N}}{(235 \text{ s}) \left(9.8 \frac{\text{m}}{\text{s}^2} \right)} = 4.34\text{E-}4 \frac{\text{kg}}{\text{s}} = 0.434 \frac{\text{g}}{\text{s}} \quad (27)$$

14.4 Effective Exhaust Velocity

$$C \left[\frac{\text{m}}{\text{s}} \right] = C^i C_F \quad (28)$$

See Appendix B ,CEA results

14.5 Specific Impulse

$$I_{sp}[s] = \frac{C}{g_o} \quad (29)$$

See Appendix B ,CEA results

14.6 BOL propellant tank pressure

$$P_{tank, BOL} = P_c + \Delta P_{dynamic} + \Delta P_{feed} + \Delta P_{inj} [Pa]$$

$$P_c = 2E6 [Pa]$$

$$\Delta P_{dynamic} = \frac{1}{2} \rho_i V^2 = \frac{1}{2} \left(1240 \frac{kg}{m^3} \right) 22.62^2 = i$$

$$\Delta P_{feed} = 50000 [Pa] (conservative)$$

$$\Delta P_{inj} = 0.2 P_c [Pa] (unthrottled)$$

Liquid

$$P_{tank, BOL} = 2.78E6 Pa$$

Gel

$$P_{tank, BOL} = 2.78E6 Pa$$

14.7 Injector Area

Liquid

Shower head

$$A_{inj} = \frac{\dot{m}}{N} \sqrt{\frac{k}{2 \rho \Delta P_{inj}}} \quad (30)$$

$$\dot{v} = \frac{4.34E-4 \frac{kg}{s}}{1} \sqrt{\frac{1.2}{2(1240 \frac{kg}{m^3})(4E5 Pa)}} = 1.509E-8 \dot{v} \quad \begin{matrix} m \\ [\dot{\dot{v}} 2] \end{matrix}$$

$$r_{inj} = 0.00693 \text{ cm}$$

$$v_{inj} = \frac{\dot{m}}{A_{inj} N \rho} \quad (31)$$

$$\dot{v} = \frac{4.34E-4 \frac{kg}{s}}{(1.509E-8 m^2) 1 (1240 \frac{kg}{m^3})} = 23.19 \left[\frac{m}{s} \right]$$

Gel

Doublet

$$A_{inj} = \frac{\dot{m}}{N} \sqrt{\frac{k}{2 \rho \Delta P_{inj}}} = \frac{4.34E-4 \frac{kg}{s}}{2} \sqrt{\frac{1.2}{2(1321 \frac{kg}{m^3})(4E5 Pa)}} = 7.312E-9 \dot{v} \quad \begin{matrix} m \\ [\dot{\dot{v}} 2] \end{matrix}$$

$$r_{per\ inj\ orifice} = 0.00242 \text{ cm}$$

Triplet

$$A_{inj} = \frac{\dot{m}}{N} \sqrt{\frac{k}{2 \rho \Delta P_{inj}}} = \frac{4.34E-4 \frac{kg}{s}}{3} \sqrt{\frac{1.2}{2(1321 \frac{kg}{m^3})(4E5 Pa)}} = 4.875E-9 \dot{v} \quad \begin{matrix} m \\ [\dot{\dot{v}} 2] \end{matrix}$$

$$r_{per\ inj\ orifice} = 0.00132 \text{ cm}$$

$$v_{inj} = \frac{\dot{m}}{A_{inj} N \rho} \quad (32)$$

$$\dot{v} = \frac{4.34\text{E-}4 \frac{\text{kg}}{\text{s}}}{(4.875\text{E-}9 \text{m}^2) 3 (1321 \frac{\text{kg}}{\text{m}^3})} = 22.46 \left[\frac{\text{m}}{\text{s}} \right]$$

A_{inj} = injector inlet cross – sectional area

N = number of injectors

k = head loss coefficient (1.2 for radiused inlet , 1.7 for nonradiused)

v_{inj} = flow velocity through injector

14.8 ΔV for Hohmann transfer

$$V_1 = \sqrt{\frac{k^2}{r_1}} \quad (33)$$

$$V_2 = \sqrt{\frac{k^2}{r_2}} \quad (34)$$

$$V_{pt} = \sqrt{\frac{2k^2}{r_1} - \frac{k^2}{a}} \quad (35)$$

$$V_{at} = \sqrt{\frac{2k^2}{r_2} - \frac{k^2}{a}} \quad (36)$$

$$a = \frac{r_1 + r_2}{2} \quad (37)$$

$$\Delta V_1 = V_{pt} - V_1 \quad (38)$$

$$\Delta V_2 = V_2 - V_{at} \quad (39)$$

$$\Delta V = \Delta V_1 + \Delta V_2 \quad (40)$$

%% Delta-V for Hohmann transfer

```
r_earth = 6371E3; % m
r_init = 450E3 + r_earth;
r_final = 650E3 + r_earth;
r_diff = r_final - r_init;
G = 6.67E-11;
```

```

M = 5.98E24;

a_transfer = (r_init + r_final) / 2;
v_init = sqrt(G*M/r_init);
v_final = sqrt(G*M/r_final);

v_tx_init = sqrt(G*M * (2 / r_init - 1 / a_transfer));
v_tx_final = sqrt(G*M * (2 / r_final - 1 / a_transfer));

delV_init = v_tx_init - v_init;
delV_final = v_final - v_tx_final;
delV_req = 2 * (delV_init + delV_final) % m/s, 2 is for the additional
inclination change

```

delV_req = 219.3937

14.9 Propellant mass

$$m_c = m_i - m_f \quad (41)$$

$$\frac{m_i}{m_f} = e^{\frac{\Delta V}{I_{sp} g_o}} \quad (42)$$

$$\Delta V = 219.3927 \left[\frac{m}{s} \right]$$

$$I_{sp} = 235 [s]$$

$$g_o = 9.81 \left[\frac{m}{s^2} \right]$$

$$m_f = 100 [kg]$$

%% Mass Ratio

```

Isp = 235;
g = 9.81;
MR = exp(delV_req/Isp/g); % mass ratio
mass_final = 100; % kg, assuming 100 kg satellite
mass_init = mass_final * MR;
mass_prop = mass_init - mass_final
mass_prop = 9.9843

```

14.10 Pressurant gas weight

$$\begin{aligned} \text{Trapped} &\propto \dot{V} + V_{\text{Boil off}} + V_{\text{Ullage}} \\ \text{Usable} &\propto \dot{V} + V_i \\ V_{\text{tank}} &= V_i \end{aligned} \quad (43)$$

$$\text{Usable} \propto \dot{V} = \frac{\dot{m}_i}{\rho_i} \quad (44)$$

$$\begin{aligned} \text{Usable} &\propto \dot{V} \\ \text{Trapped} &\propto \dot{V} = (1 - \eta_{\text{expulsion}}) \cdot V_i \end{aligned} \quad (45)$$

$$V_{\text{BoilOff}} = 0 \text{ (only applicable for cryogenic propellants)} \quad (46)$$

$$\begin{aligned} \text{Trapped} &\propto \dot{V} \\ \text{Usable} &\propto \dot{V} \cdot V_i \end{aligned} \quad (47)$$

$$V_{\text{Ullage}} = (\text{Ullage Percentage}) \dot{V}$$

$$W_g = \frac{P_T V_T}{R_g T_g} = \frac{(2E6 \frac{kg}{m \cdot s^2})(V_{\text{tank}} m^3)}{(R_g)(283 K)}$$

$$\text{Helium } R_g = 2077 \frac{m^2}{s^2 * K} \rightarrow W_g = kg$$

R_g values (The Individual and Universal Gas Constant)
(Huzel & Huang, 1967)

%% Pressurant Weight

```
rho_prop = 1240; % kg/m^3
pressure_tank = 2E6; % Pa
Rg = 2077; % m^2 / s^2*K
Tg = 283; % K
```

% Propellant tank volume

```
vol_boil_off = 0; % cryogenics only
vol_usable_prop = mass_prop / rho_prop; % m^3
eff_expulsion = 0.90; % assumed/goal
vol_trapped_prop = (1-eff_expulsion) * vol_usable_prop;
ullage_percentage = 0.025;
vol_ullage = ullage_percentage * (vol_usable_prop + vol_trapped_prop);
```

```
vol_tank = vol_usable_prop + vol_trapped_prop + vol_boil_off +  
vol_ullage
```

```
Wg = (pressure_tank * vol_tank) / (Rg * Tg) % kg
```

Wg = 0.0309 [kg]

```
%% For 0.5L testbed
```

```
% Simulant properties
```

```
rho_sim = 1019.06; % kg/m^3
```

```
% Propellant tank volume
```

```
vol_tank = 0.0005; % m^3
```

```
pressure_tank_bol = 2000000; % Pa
```

```
pressure_tank_eol = 550000; % Pa
```

```
% Weight of the gas pressurant at EOL
```

```
Wg_testbed = (pressure_tank_eol * vol_tank) / (Rg * Tg) % ideal gas law,  
kg
```

```
% Based on EOL pressure, the mass of the BOL propellant mass/volume is  
% found
```

```
vol_tank_pressurant = (Wg_testbed * Rg * Tg) / pressure_tank_bol; % m^3,
```

```
volume of 0.5L tank that gas takes up to pressurize to 2E6 Pa at BOL
```

```
vol_prop_bol = vol_tank - vol_tank_pressurant % simulant volume to be  
used;
```

```
mass_prop_bol = vol_prop_bol * rho_sim % kg
```

vol_prop_bol = 3.6250e-04

mass_prop_bol = 0.3694

14.11 Vane weight

```
%% PMD Weight
close all; clear all; clc;

%% Single, simple vane for CFD model
% Estimated dimensions (m)

t = 0.002;
h = 0.04;
L = 0.5315;

V = t * h * L;

% 304L stainless steel, g/m^3
rho_304L = 8030000;

vane_weight = rho_304L * V

% Added propellant space

rho_prop_liq = 1240; % kg/m^3
rho_prop_gel = 1321; % kg/m^3

extra_liq = V*rho_prop_liq
extra_gel = V*rho_prop_gel
```

vane_weight = 341.4356 g

extra_liq = 0.0527

extra_gel = 0.0562

15 Appendix B - LMP-103S Propellant Verification

15.1 Mixture Properties

Property	LMP-103S	Mixture 1	Mixture 2	Mixture 3
Density (kg/m ³)*	1240	1013	1019.06	1046.8
Dynamic Viscosity (Pa·s)*	0.0033-0.003	0.00595	0.00513	0.00544
Surface Tension (N/m)	0.03	0.0373	0.040	----

Table 7: Mixture liquid properties
* 20 - 25°C

Property	Mixture 1	Mixture 2	Mixture 3*
Density (kg/m ³)	1094	1071.11	----
Dynamic Viscosity (Pa·s)*	Infinite ⁺	Infinite ⁺	----
Surface Tension (N/m)	0.07063	0.0700	----

Table 8: Mixture gel properties
* Not investigated further
+ Tested time was > 20 mins

15.2 Combustion Properties

Chemical Compound	Molecular Formula	Liquid Mass %	Gel Mass %
ADN	C ₂ H ₃ O ₂ NH ₄	65	61.9

Methanol	CH ₃ OH	20	19.1
Ammonia	NH ₃	6	5.7
Water	H ₂ O	9	8.6
Cab-O-Sil	SiO ₂	----	4.7
O/F	----	2.85	3.04

Figure 24: Liquid and gel mixture amounts using actual LMP-103S mass percentages

		Molecular Formula	ΔH^o_f (kJ/mol) *	Incoming temperature to combustion chamber (K)	Combustion Temperature⁺ (K)
Fuel	Methanol	CH ₃ OH	-238.6	308	1881
	Ammonia	NH ₃	-80.8	239	1881
Oxidizer	Water	H ₂ O	-285.8	308	1881
	ADN	NH ₄ N(NO ₂) ₂	134.6	308	1881
	Cab-O-Sil	SiO ₂	-911	308	1881

Figure 25: CEA gel combustion variables

15.3 NASA CEA Analysis

15.3.1 Program Results

15.3.1.1 Liquid

 NASA-GLENN CHEMICAL EQUILIBRIUM PROGRAM CEA2, MAY 21, 2004
 BY BONNIE MCBRIDE AND SANFORD GORDON
 REFS: NASA RP-1311, PART I, 1994 AND NASA RP-1311, PART II, 1996

problem case=0012 o/f=2.85,
 rocket equilibrium frozen nfz=1 t,k=1881
 p,bar=3,

```

pi/p=3,
react
fuel=CH3OH(L) wt=20 t,c=35
fuel=NH3(L) wt=6 t,c=-34
oxid=H2O(L) wt=9 t,c=35
oxid=ADN wt=65 t,c=35 N 1 H 4 N 1 N 1 O 2
only
CO CO2 H2 H2O N2
output massf transport
plot p t rho h u g s m mw cp gam son pip mach aeat cf ivac isp vis
end

```

```

OPTIONS: TP=F HP=F SP=F TV=F UV=F SV=F DETN=F SHOCK=F REFL=F
INCD=F
RKT=T FROZ=T EQL=T IONS=F SIUNIT=T DEBUGF=F SHKDBG=F DETDBG=F
TRANSPT=T

```

T,K = 1881.0000

TRACE= 0.00E+00 S/R= 0.000000E+00 H/R= 0.000000E+00 U/R= 0.000000E+00

Pc,BAR = 3.000000

Pc/P = 3.0000

SUBSONIC AREA RATIOS =

SUPERSONIC AREA RATIOS =

NFZ= 1 Mdot/Ac= 0.000000E+00 Ac/At= 0.000000E+00

REACTANT	WT.FRAC	(ENERGY/R),K	TEMP,K	DENSITY
EXPLODED FORMULA				
F: CH3OH(L)	0.769231	-0.286354E+05	308.15	0.0000
C 1.00000	H 4.00000	O 1.00000		
F: NH3(L)	0.230769	-0.860604E+04	239.15	0.0000
N 1.00000	H 3.00000			
O: H2O(L)	0.121622	-0.342866E+05	308.15	0.0000
H 2.00000	O 1.00000			
O: ADN	0.878378	0.000000E+00	308.15	0.0000
N 1.00000	H 4.00000	N 1.00000	N 1.00000	O 2.00000

SPECIES BEING CONSIDERED IN THIS SYSTEM
(CONDENSED PHASE MAY HAVE NAME LISTED SEVERAL TIMES)
LAST thermo.inp UPDATE: 9/09/04

```

tpis79 *CO          g 9/99 *CO2          tpis78 *H2
g 8/89 H2O         tpis78 *N2

```

SPECIES WITH TRANSPORT PROPERTIES

PURE SPECIES

```

CO          CO2          H2          H2O
N2

```

BINARY INTERACTIONS

CO CO2
 CO N2
 CO2 H2
 CO2 H2O
 CO2 N2
 H2 H2O
 H2 N2
 H2O N2

O/F = 2.850000

	EFFECTIVE FUEL	EFFECTIVE OXIDANT	MIXTURE
ENTHALPY	h(2)/R	h(1)/R	h0/R
(KG-MOL)(K)/KG	-0.80406686E+03	-0.23146993E+03	-0.38019641E+03

KG-FORM.WT./KG	bi(2)	bi(1)	b0i
C	0.24007057E-01	0.00000000E+00	0.62355993E-02
H	0.13667923E+00	0.58517860E-01	0.78819514E-01
O	0.24007057E-01	0.29258930E-01	0.27894807E-01
N	0.13550334E-01	0.33761856E-01	0.28512110E-01

POINT	ITN	T	C	H	O	N
1	6	1881.000	-12.644	-9.666	-23.314	-13.537
Pinf/Pt = 1.803674						
2	3	1668.018	-11.922	-9.770	-25.179	-13.636
Pinf/Pt = 1.807921						
2	2	1667.212	-11.919	-9.771	-25.187	-13.636
3	3	1501.004	-11.178	-9.862	-27.039	-13.725

THEORETICAL ROCKET PERFORMANCE ASSUMING FROZEN COMPOSITION
 AT AN ASSIGNED TEMPERATURE

Pin = 228.1 PSIA
 CASE = 0012

REACTANT	WT FRACTION	ENERGY	TEMP
	(SEE NOTE) KJ/KG-MOL	K	
FUEL CH3OH(L)	0.7692308	-238089.481	308.150
FUEL NH3(L)	0.2307692	-71555.000	239.150
OXIDANT H2O(L)	0.1216216	-285076.537	308.150
OXIDANT ADN	0.8783784	0.000	308.150

O/F= 2.85000 %FUEL= 25.974026 R,EQ.RATIO= 1.859879 PHI,EQ.RATIO= 0.000000

CHAMBER THROAT EXIT

Pinf/P 1.0000 1.8114 15.730
P, BAR 15.730 8.6837 1.0000
T, K 1881.00 1663.96 1031.92
RHO, KG/CU M 1.6791 0 1.0478 0 1.9457-1
H, KJ/KG -2577.93 -3101.90 -4532.33
U, KJ/KG -3514.77 -3930.64 -5046.28
G, KJ/KG -27803.2 -25416.5 -18371.0
S, KJ/(KG)(K) 13.4106 13.4106 13.4106

M, (1/n) 16.694 16.694 16.694
Cp, KJ/(KG)(K) 2.4455 2.3810 2.1307
GAMMAS 1.2557 1.2645 1.3051
SON VEL, M/SEC 1084.6 1023.7 819.0
MACH NUMBER 0.000 1.000 2.414

TRANSPORT PROPERTIES (GASES ONLY)
CONDUCTIVITY IN UNITS OF MILLIWATTS/(CM)(K)

VISC, MILLIPOISE 0.66406 0.60879 0.42993

WITH FROZEN REACTIONS

Cp, KJ/(KG)(K) 2.4455 2.3810 2.1307
CONDUCTIVITY 2.6710 2.3794 1.5228
PRANDTL NUMBER 0.6080 0.6092 0.6016

PERFORMANCE PARAMETERS

Ae/At 1.0000 2.7884
CSTAR, M/SEC 1466.5 1466.5
CF 0.6981 1.3482
Ivac, M/SEC 1833.2 2237.0
Isp, M/SEC 1023.7 1977.1

MASS FRACTIONS

*CO 0.13874 *CO2 0.05644 *H2 0.03837
H2O 0.36709 *N2 0.39936

* THERMODYNAMIC PROPERTIES FITTED TO 20000.K

PRODUCTS WHICH WERE CONSIDERED BUT WHOSE MASS FRACTIONS
WERE LESS THAN 5.000000E-06 FOR ALL ASSIGNED CONDITIONS

NOTE. WEIGHT FRACTION OF FUEL IN TOTAL FUELS AND OF OXIDANT IN TOTAL
OXIDANTS

15.3.1.2 Gel

NASA-GLENN CHEMICAL EQUILIBRIUM PROGRAM CEA2, MAY 21, 2004
BY BONNIE MCBRIDE AND SANFORD GORDON
REFS: NASA RP-1311, PART I, 1994 AND NASA RP-1311, PART II, 1996

problem case=0016 o/f=3.04,
rocket equilibrium frozen nfz=1 t,k=1881
p,bar=3,
pi/p=3,
react
fuel=CH3OH(L) wt=19.1 t,c=35
fuel=NH3(L) wt=5.7 t,c=-34
oxid=H2O(L) wt=8.6 t,c=35
oxid=SiO2(a-qz) wt=4.7 t,c=35
oxid=ADN wt=61.9 t,c=35
h,kj/mol=134.6 N 1 H 4 N 1 N 1 O 2
omit
Si(cr) Si(L) SiC(b) SiC(L) SiO2(a-qz) SiO2(b-qz) SiO2(b-crt) SiO2(L)
Si2N2O(cr) Si3N4(cr)
output transport
plot p t rho h u g s m mw cp gam son pip mach aeat cf ivac isp vis
end

OPTIONS: TP=F HP=F SP=F TV=F UV=F SV=F DETN=F SHOCK=F REFL=F
INCD=F
RKT=T FROZ=T EQL=T IONS=F SIUNIT=T DEBUGF=F SHKDBG=F DETDBG=F
TRANSPT=T

T,K = 1881.0000

TRACE= 0.00E+00 S/R= 0.000000E+00 H/R= 0.000000E+00 U/R= 0.000000E+00

Pc,BAR = 3.000000

Pc/P = 3.0000

SUBSONIC AREA RATIOS =

SUPERSONIC AREA RATIOS =

NFZ= 1 Mdot/Ac= 0.000000E+00 Ac/At= 0.000000E+00

REACTANT	WT.FRAC	(ENERGY/R),K	TEMP,K	DENSITY
F: CH3OH(L)	0.770161	-0.286354E+05	308.15	0.0000
EXPLODED FORMULA				
C	1.00000	H 4.00000	O 1.00000	
F: NH3(L)	0.229839	-0.860604E+04	239.15	0.0000
N	1.00000	H 3.00000		
O: H2O(L)	0.114362	-0.342866E+05	308.15	0.0000
H	2.00000	O 1.00000		
O: SiO2(a-qz)	0.062500	-0.109477E+06	308.15	0.0000
Si	1.00000	O 2.00000		
O: ADN	0.823138	0.161886E+05	308.15	0.0000
N	1.00000	H 4.00000	N 1.00000	N 1.00000
		O 2.00000		

SPECIES BEING CONSIDERED IN THIS SYSTEM
(CONDENSED PHASE MAY HAVE NAME LISTED SEVERAL TIMES)
LAST thermo.inp UPDATE: 9/09/04

SPECIES WITH TRANSPORT PROPERTIES

PURE SPECIES

C	CH4	CH3OH	CO
CO2	C2H2,acetylene		
C2H4	C2H6	C2H5OH	C2N2
H	HCN		
H2	H2O	N	NH3
NO	NO2		
N2	N2O	N2O4	O
OH	O2		
SiH4			

BINARY INTERACTIONS

C	O
CH4	O2
CO	CO2
CO	N2
CO	O2
CO2	H2
CO2	H2O
CO2	N2
CO2	O2
H	H2
H	N
H	N2
H	O
H2	H2O
H2	N2
H2	O2
H2O	N2
H2O	O2
N	NO
N	N2
N	O
N	O2
NO	O
N2	O
N2	O2
O	O2

O/F = 3.040000

	EFFECTIVE FUEL	EFFECTIVE OXIDANT	MIXTURE
ENTHALPY	h(2)/R	h(1)/R	h0/R
(KG-MOL)(K)/KG			
	-0.80442824E+03	-0.16080367E+03	-0.32011668E+03
KG-FORM.WT./KG	bi(2)	bi(1)	b0i
*C	0.24036098E-01	0.00000000E+00	0.59495292E-02
*H	0.13663148E+00	0.54880900E-01	0.75116192E-01
*O	0.24036098E-01	0.29520860E-01	0.28163246E-01

*N 0.13495695E-01 0.31638616E-01 0.27147794E-01
 *Si 0.00000000E+00 0.10402052E-02 0.78272865E-03

POINT	ITN	T	C	H	O	N
		Si				
1	20	1881.000	-12.748	-9.693	-23.239	-13.544
		-15.739				
Pinf/Pt = 1.801308						
2	3	1670.513	-12.043	-9.798	-25.080	-13.645
		-14.864				
Pinf/Pt = 1.806514						
2	2	1669.529	-12.040	-9.799	-25.089	-13.645
		-14.859				
3	3	1503.924	-11.309	-9.891	-26.929	-13.735
		-13.953				

THEORETICAL ROCKET PERFORMANCE ASSUMING FROZEN COMPOSITION
 AT AN ASSIGNED TEMPERATURE

Pin = 43.5 PSIA
 CASE = 0016

REACTANT	WT FRACTION (SEE NOTE)	ENERGY KJ/KG-MOL	TEMP K
FUEL CH3OH(L)	0.7701613	-238089.481	308.150
FUEL NH3(L)	0.2298387	-71555.000	239.150
OXIDANT H2O(L)	0.1143617	-285076.537	308.150
OXIDANT SiO2(a-qz)	0.0625000	-910249.267	308.150
OXIDANT ADN	0.8231383	134600.000	308.150

O/F= 3.04000 %FUEL= 24.752475 R, EQ. RATIO= 1.811674 PHI, EQ. RATIO=
 0.000000

	CHAMBER	THROAT	EXIT
Pinf/P	1.0000	1.8104	3.0000
P, BAR	3.0000	1.6571	1.0000
T, K	1881.00	1665.12	1497.05
RHO, KG/CU M	3.3146-1	2.0682-1	1.3883-1
H, KJ/KG	-2666.81	-3172.71	-3556.65
U, KJ/KG	-3571.88	-3973.92	-4276.99
G, KJ/KG	-28751.8	-26264.0	-24317.1
S, KJ/(KG)(K)	13.8676	13.8676	13.8676

M, (1/n)	17.280	17.280	17.280
Cp, KJ/(KG)(K)	2.3736	2.3116	2.2560
GAMMAS	1.2543	1.2629	1.2711
SON VEL, M/SEC	1065.5	1005.9	956.9
MACH NUMBER	0.000	1.000	1.394

TRANSPORT PROPERTIES (GASES ONLY)
 CONDUCTIVITY IN UNITS OF MILLIWATTS/(CM)(K)

VISC, MILLIPOISE 0.66797 0.61264 0.56780

WITH FROZEN REACTIONS

Cp, KJ/(KG)(K) 2.3736 2.3116 2.2560
CONDUCTIVITY 2.6012 2.3178 2.0946
PRANDTL NUMBER 0.6095 0.6110 0.6116

PERFORMANCE PARAMETERS

Ae/At 1.0000 1.1233
CSTAR, M/SEC 1442.0 1442.0
CF 0.6975 0.9251
Ivac, M/SEC 1802.4 1874.0
Isp, M/SEC 1005.9 1334.1

MOLE FRACTIONS

*CO	0.08036	*CO2	0.02244	*H	0.00022
*H2	0.30115	H2O	0.34772	NH3	0.00001
*N2	0.23455	*OH	0.00002	SiO	0.01338
SiO2	0.00014				

* THERMODYNAMIC PROPERTIES FITTED TO 20000.K

NOTE. WEIGHT FRACTION OF FUEL IN TOTAL FUELS AND OF OXIDANT IN TOTAL OXIDANTS

15.3.2 R-Squared Determination

15.3.2.1 Matlab Results

```
close all, clear all, clc
```

```
Pc = [24.5 22 16 10.5 7 5.5 3];  
ecaps_isp = [2280 2260 2220 2180 2080 2010 1880];
```

```
% Liquid  
% cea_isp = [2305.9 2290 2240 2166.6 2088 2037.6 1905.9]
```

```
% Gel  
cea_isp = [2268.4 2252.7 2203.4 2131.0 2053.4 2003.8 1874]
```

```
% Squared error of cea_isp to ecaps_isp  
residual_error = ecaps_isp - cea_isp;  
SE_line = sum(residual_error.^2)  
y_avg = sum(ecaps_isp)/length(ecaps_isp)
```

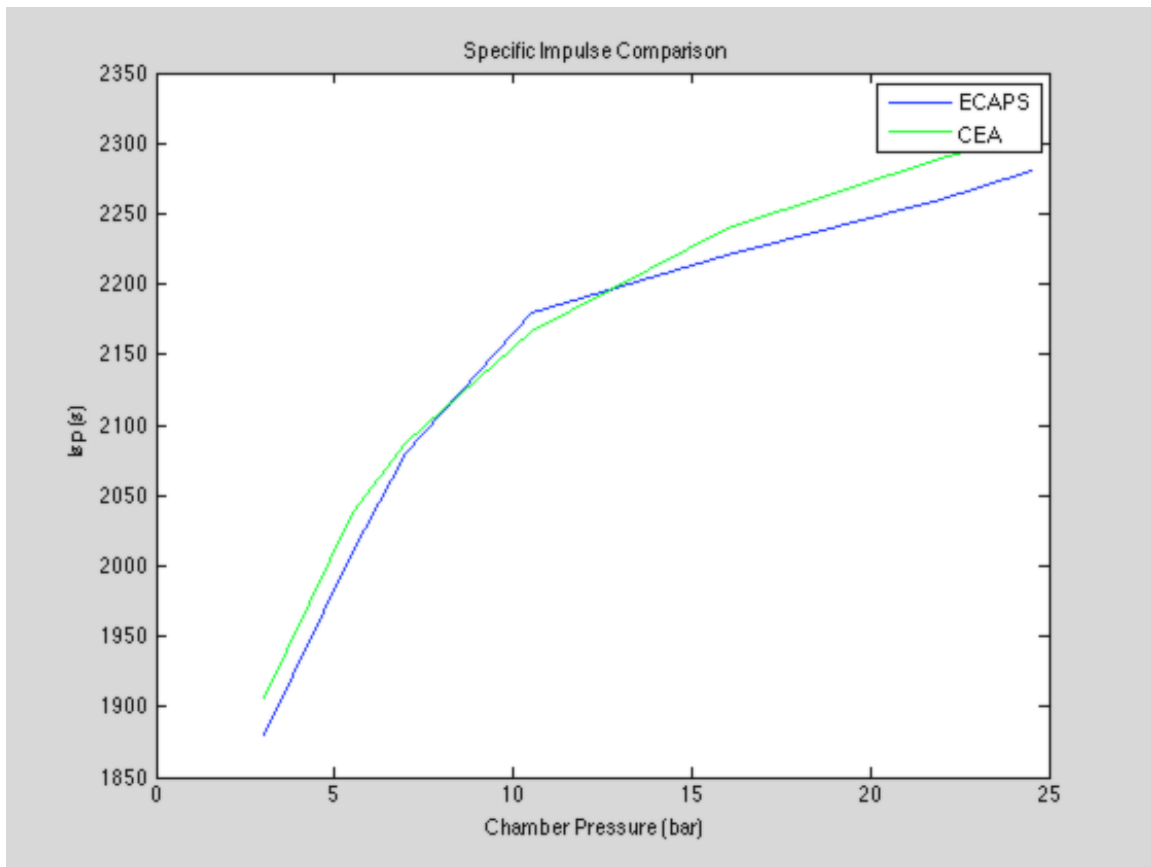
```
% Squared error of cea_isp to ecaps_isp y_avg  
y_avg_variation_error = cea_isp - y_avg;  
y_variation = sum(y_avg_variation_error.^2);  
r_squared = 1 - SE_line/y_variation
```

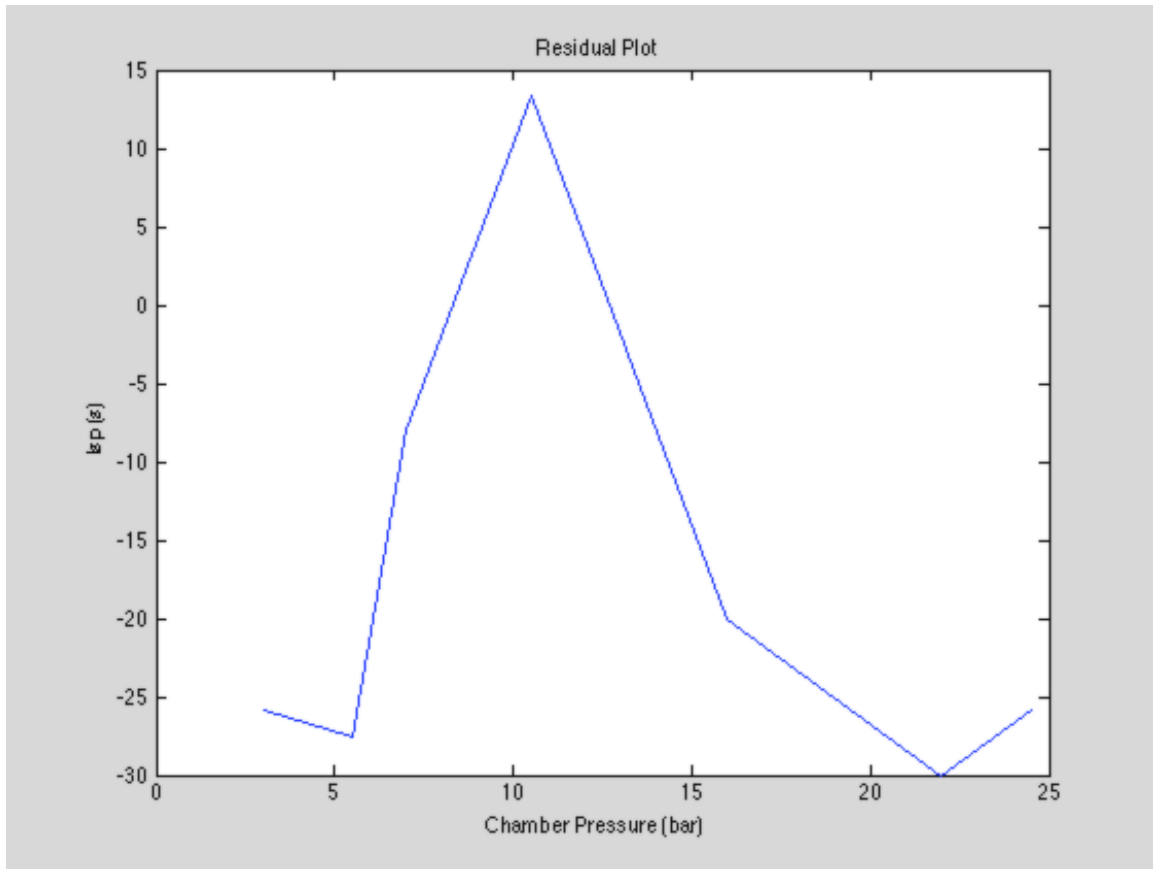
```
figure(1)
```

```
plot(Pc, ecaps_isp, Pc, cea_isp, 'g')
legend('ECAPS', 'CEA')
title('Specific Impulse Comparison')
ylabel('Isp (s)')
xlabel('Chamber Pressure (bar)')
```

```
figure(2)
plot(Pc, residual_error)
title('Residual Plot')
ylabel('Isp (s)')
xlabel('Chamber Pressure (bar)')
```

r_squared = 0.9721





Chamber Pressure (bar)	Liquid CEA derived I_{sp} with O/F = 2.85 Ns/kg (s)	Gel CEA derived I_{sp} with O/F = 3.04 Ns/kg (s)	ECAPS Results (Approx., Ns/kg)
3	1905.9 (194.3)	1874 (191.0)	1880
5.5	2037.6 (207.7)	2003.8 (204.3)	2010
7	2088.0 (212.8)	2053.4 (209.3)	2080
10.5	2166.6 (220.9)	2131.0 (217.2)	2180
16	2240.0 (228.3)	2203.4 (224.6)	2220
22	2290.0 (233.4)	2252.7 (229.6)	2260
24.5	2305.9 (235.1)	2268.4 (231.2)	2280
R^2 value	0.9721	0.9713	

Table 9: * Low mixture